U.PORTO
FEUP FACULDADE DE ENGENHARIA UNIVERSIDADE DO PORTO
TU Delft

Is ammonia removal hindered by iron in rapid sand filters?

Interactions between iron oxides, reactive oxygen species, and ammonia-oxidizing microorganisms

Sofia Maria de Melo Malheiro

Dissertation submitted for the degree of
MASTER IN BIOENGINEERING

Partnership provided by Erasmus+ Internship Program

Supervisor at TU Delft
Prof. dr. ir. Mark van Loosdrecht

Co-Supervisors at TU Delft
Ir. Francesc Corbera Rubio
Dr. Michele Laureni
Dr. ir. Doris van Halem

Supervisor at FEUP
Prof. Dr. Luís Melo

July, 2022

Abstract

Rapid Sand Filtration (RSF) is used to produce Drinking Water (DW) from Groundwater. It comprises the oxidation and removal of groundwater's three most common inorganic contaminants - iron, ammonia, and manganese. Usually, iron is entirely removed in the top part of RSF, whereas ammonia only starts to get oxidized after iron is no longer present. The reason for this phenomenon is not understood. Thus, in this work, the role of iron-(hydro)oxides (FeOx) coating the sand grains of the filter media and the formation of reactive oxygen species (ROS) in ammonia oxidation will be evaluated. To this end, three main set-ups were studied: (1) the colonization of three lab-scale RSF columns comprising FeOx-coating and virgin quartz sand as a filter media; (2) the monitoring of ammonia oxidation rates in the presence of iron(II) and ROS scavengers with batch tests; and (3) the recovery profile of a lab-scale column with total ammonia removal capacity after iron(II) addition. Results showed that, despite the several attempts to colonize virgin quartz sand, inoculation was only successful after the presence of iron oxides, leading to the belief that mineral oxides might be a critical factor in the ripening of RSF. Contrarily, the FeOx-coated sand column achieved complete ammonia removal after the 11th day of continuous flow, whereas 29 days were necessary for FeOx-virgin sand column to reach it. Furthermore, batch tests results indicate that ROS are not responsible for iron-caused inhibition of ammonia oxidation since scavengers could not neutralize the hindrance. Lastly, the ammonia removal profile did not recover after being submitted to a one-day continuous inflow of 3 mg/L of Fe^{2+}, suggesting that the new layer of FeOx could be the underlying reason for the inhibition.

Keywords: rapid sand filtration, ammonia oxidation, iron oxidation, iron-(hydro)oxides, reactive oxygen species, ammonia-oxidizing microorganisms

Acknowledgements

First, on a more academic and professional note,

I would like to thank all the professors who have taught me over the past years, and to FEUP, for being a faculty I am honoured to call home.

To Prof. Dr. Luís Melo, for supervising me and providing me with the opportunity to come to TU Delft.

To Prof. Dr. Mark van Loosdrecht, for accepting me into his research group and granting me a research topic.

To PhD candidate Francesc Corbera Rubio, for all his daily supervising, discussion, and advice on how to improve my research.

To Prof. Dr. Michele Laureni and Prof. Dr. Doris van Halem, for all their insights and fresh ideas on tackling the problem.

Second, on a more familiar note,

To my dear boyfriend José Carlos Coutinho, for enduring and supporting me over these past five months and learning how to deal with my anxiety. Thank you for caring so much, helping me with everything you could, and making me feel complete.

To my dear mother, Maria José Melo, for all her patience, compassion, and support, especially in my bad moments. Thank you for teaching me how to cope with my feelings.

To my dear father, Luís Malheiro, who always inspired me to be better, curious, and critical. Thank you for teaching me that there's a whole world to understand and that we know very little about it.

To both of you, thank you for raising me and making me the person I am today. I would not be here if it weren't for your unconditional love and guidance.

To my dear 'not-so-younger' brother, André Malheiro, who may not believe, but has taught me a lot about balance, stability, and self-improvement. Thank you for being a pillar in my life.

To my dear aunt, Maria Amélia Malheiro, for all her support and mentoring about empathy and the importance of being observant. Thank you for encouraging me to reach wherever I want.

To all my family for the happy gatherings, summer holidays on the beach, and unwinding moments. Thank you for making my life more joyful.

Third, on a more "Chill-autus" note,

To all the friends I made as part of "Tuna Feminina de Engenharia". Thank you for all those years of companionship and bohemianism. Thank you for believing in me and, above all, for making these years in college the best ones I could dream of.

I finish this Master's degree happier than I could ever be, and, surely, it is mainly because all of you.

"The important thing is not to stop questioning.
Curiosity has its own reason for existing."

- Albert Einstein

Contents

1 Introduction **1**
- 1.1 Context . . . 1
  - 1.1.1 The importance of Water . . . 1
  - 1.1.2 The Dutch Approach . . . 2
- 1.2 Addressing Problem . . . 3
- 1.3 Outline of the Thesis . . . 6

2 Literature Review **7**
- 2.1 Rapid Sand Filtration . . . 7
- 2.2 Iron oxidation . . . 8
  - 2.2.1 Iron Oxides . . . 9
  - 2.2.2 Reactive Oxygen Species . . . 10
- 2.3 Ammonia oxidation . . . 12
  - 2.3.1 The Nitrogen Cycle . . . 12
  - 2.3.2 Nitrifiers . . . 14
- 2.4 Possible interactions between species . . . 16
  - 2.4.1 Iron oxides and ammonia-oxidizing microorganisms . . . 16
  - 2.4.2 ROS and ammonia-oxidizing microorganisms . . . 16

3 Materials and Methods **19**
- 3.1 Columns Start-up . . . 19
- 3.2 Columns Tests . . . 20
  - 3.2.1 Evaluating the role of FeOx-coated sand on the process of ammonia oxidation . . . 21
  - 3.2.2 Evaluating the effect of iron(II) addition into the system . . . 21
- 3.3 Batch Tests . . . 21
  - 3.3.1 Evaluation of iron(II) addition . . . 21
  - 3.3.2 Evaluation of ROS quenchers addition . . . 22
- 3.4 Analytical Procedures . . . 22

4 Results and Discussion **23**
- 4.1 Columns ripened exclusively in the presence of FeOx-coated sand . . . 23
- 4.2 FeOx-coating as a possible key to microbial development in RSF . . . 24
- 4.3 Reactive Oxygen Species are not responsible for ammonia oxidation inhibition . . . 27
  - 4.3.1 Iron(II) additions inhibit the maximum ammonia removal rate 27
  - 4.3.2 ROS quenchers do not prevent inhibition . . . 27
- 4.4 Adsorption of newly formed iron oxides can disturb the microbial community . . . 29

5 Conclusions **31**

6 Future Recommendations **33**

References **37**

A Appendix **A**
A.1 Columns Design and Filter Media . . . . . A
A.2 Hammerflier LOW filter sand activity . . . . . B
A.3 Composition of Trace Elements Solution . . . . . B
A.4 Columns Sampling Procedure . . . . . B

B Appendix **C**
B.1 Column's ammonia removal capacity profiles C
B.2 FeOx-virgin sand column's virgin quartz sand's ammonia oxidation activity . . . . . D
B.3 Iron(II) addition batch tests . . . . . D
B.4 Tempol, mannitol, and catalase interference with ammonia oxidation process . . . . . E

List of Figures

1.1 Drinking water production sources in the Netherlands. Retrieved from (Smeets et al., 2009). 2
1.2 Schematic representation of a conventional groundwater treatment system. Retrieved from (de Vet et al., 2010). 3
1.3 Evolution of ammonia and iron(II) concentrations at different stages of the production of Drinking Water in five different Drinking Water Treatment Plants in the Netherlands - Hasselo (a), Druten (b), Breehei (c) and (d), and Culemborg (d). The samples were withdrawn before the aeration step (Raw Water), after the aeration step (AA) and at different filter heights (F1, F2, F3, F4, F5, and F6). In figures (a) and (b), only raw water and effluents of two consecutive filters were measured. 5

2.1 Contribution of the iron(II) oxidation processes to Rapid Sand Filtration as a function of pH. Retrieved from (van Beek et al., 2016). . 9
2.2 Schematic representation of interfacial mechanisms of Fenton systems: 1) homogeneous Fenton induced by surface leached-iron and 2) heterogeneous Fenton and Fenton-like catalysis. Retrieved from (He et al., 2016). 12
2.3 The Nitrogen Cycle, with each pathway represented in different colors. The oxidation state of nitrogen in each of the intermediates is outlined inside the grey circles. Based on Stein et al., 2016 13

3.1 Schematic representation of start-up strategy in the columns. Virgin quartz sand column on the left, FeOx-virgin sand column in the middle, and FeOx-coated sand column on the right. 19
3.2 Lab-scale rapid sand filtration columns used throughout this Thesis. . 20

4.1 Timeline of the 25 days of the inoculation procedure. Light orange lines represent the time of each inoculation, whereas the red, yellow, and green bars represent the period of ammonia consumption of FeOx-coated sand, FeOx-virgin sand, and Virgin quartz sand columns, respectively. 23
4.2 Layer of activated sludge formed on virgin quartz sand column after the second inoculation. 24
4.3 (a) Full ammonia removal evolution of FeOx-coated sand (red) and FeOx-virgin sand (yellow) columns throughout experiment time, and (b) Bed height of FeOx-coated sand (red) and FeOx-virgin sand (yellow) columns at which 40% ammonia removal is achieved throughout time 25

4.4 Difference of microscopical pictures from FeOx-virgin sand column containing adsorbed iron oxides (a) and from virgin quartz sand column containing no oxides adsorption (b). 25
4.5 Evolution of the ammonia removal capacity of virgin quartz sand column's mid-height and effluent after the influent swap. 26
4.6 Consumption of ammonium throughout the experimental time between conditions control (black) and addition of iron(II) every 30 minutes (brown). * represents a statistically significant difference of $p<0.05$. 27
4.7 Ammonium consumption rates of all conditions tested. * represents a statistically significant difference of $p<0.05$, and ** a statistically significant difference of $p<0.0001$. 28
4.8 FeOx-virgin sand column's ammonia removal profile before (black), during (red), and after (shades of green) iron(II) addition. 29

6.1 Confocal Laser Scanning Micrograph showing microbial colonization of a sand grain stained with Live/Dead BacLight viability kit (top pictures, outer periphery of the grain; retrieved from Gülay et al., 2014) and with a SYBR green I stain (bottom picture; retrieved from Probandt et al., 2018). 34
6.2 Environmental Scanning Electron Micrograph showing microbial colonization of internal pores of a sand grain. Coccoid cell-like structures are indicated by arrows and numbers. Retrieved from Gülay et al., 2014. 34

A.1 Design of one column ordered from *Lenntech B.V.* as an example. Dimensions are not to scale. . . . . A
A.2 Example of the sands used as a filter media in the columns. . . . . A
A.3 Ammonia oxidation activity of Hammerflier LOW filter sand. . . . . B

B.1 Evolution of the ammonia removal capacity profiles of the lab-scale rapid sand filters columns throughout 4 weeks. C
B.2 FeOx-virgin sand column's virgin quartz sand's ammonia oxidation activity. . . . . D
B.3 Ammonia consumption throughout time in the presence of iron alone (a) and coupled with ROS quenchers Tempol (b), Mannitol (c), and Catalase (d). * represents a statistically significant difference of $p<0.05$, and ** a statistically significant difference of $p<0.0001$. . . . F
B.4 Ammonia consumption evolution time between the batch with the presence of iron and the batches with presence of iron together with ROS quenchers tempol (a), mannitol (b), and catalase (c). * represents a statistically significant difference of $p<0.05$. . . . . G
B.5 Differences in ammonia consumption throughout 4 hours of experiment between the control condition and the control with addition of tempol (a), mannitol (b), and catalase (c). * represents a statistically significant difference of $p<0.05$. . . . . H

List of Tables

1.1 Oxidizing microorganisms of iron, ammonium and manganese for groundwater treatment (de Vet et al., 2010; Madigan et al., 2019). . . 4

2.1 Overall chemical reactions of homogeneous, heterogeneous, and biological iron(II) oxidation. Adapted from (van Beek et al., 2016; van Beek et al., 2012). 8
2.2 Different types of iron oxides. Retrieved from (Cornell et al., 2003). . 10

B.1 Ammonium consumption rate of control and iron(II) addition every 30 min. The right columns indicate the Standard Deviation (SD) of the replicates and the r^2 of the linear regression used to calculate the consumption rates. . . . . D
B.2 Ammonium consumption rate of controls and the four testing conditions - addition of iron, and addition of iron together with ROS quenchers tempol, mannitol, and catalase. The right columns indicate the Standard Deviation (SD) of the replicates and the r^2 of the linear regression used to calculate the consumption rates. . . . . E

Abbreviations

AMO	Ammonia Monooxygenase
AOA	Ammonia-Oxidizing Archaea
AOB	Ammonia-Oxidizing Bacteria
AOM	Ammonia-Oxidizing Microorganisms
DO	Dissolved Oxygen
DW	Drinking Water
DWTP	Drinking Water Treatment Plant
FeOx	Iron Oxides
HAO	Hydroxylamine Oxidoreductase
NXR	Nitrite Oxidoreductase
ROS	Reactive Oxygen Species
RSF	Rapid Sand Filter / Rapid Sand Filtration
SDG	Sustainable Development Goal
SSF	Slow Sand Filter / Slow Sand Filtration
UN	United Nations
VSS	Volatile Suspended Solids
WHO	World Health Organization
WTP	Water Treatment Plant
WWTP	Wastewater Treatment Plant

Chapter 1

Introduction

This Thesis was conducted under Erasmus+ Internship Program at Delft University of Technology (*Technische Universiteit Delft*).

For approximately five months, the Master's student worked in the Environmental Biotechnology research section of the Department of Biotechnology (Faculty of Applied Sciences) partnered with the Department of Sanitary Engineering (Faculty of Civil Engineering), under the direct supervision of Francesc Corbera Rubio, PhD candidate, Michele Laurini and Doris van Halem, Assistant and Associate Professors from the Department of Civil Engineering, respectively, and Professor Mark van Loosdrecht, Full Professor and Section Leader of the Environmental Biotechnology Group.

The project is financed by the RedOx Filter project, a partnership between NWO (*Nederlandse Organisatie voor Wetenschappelijk Onderzoek*, the Dutch Research Council) and two dutch water companies, Vitens and Dunea, that seek to optimize Rapid Sand Filtration.

Thus, this Master's Thesis aims to provide an understanding of a current limitation to optimizing Rapid Sand Filtration and give some valuable knowledge into the literature. Specifically, it seeks to understand what is limiting ammonia oxidation and if that limitation might be related to the presence of iron(II) in the system.

1.1 Context

1.1.1 The importance of Water

Water is crucial to life, and, according to the World Health Organization (WHO), an adequate, safe, and accessible supply is essential for human health and should be available to all (WHO, 2017; 2022).

As contaminated water is linked to the transmission of a wide range of diseases, appropriate management and assessment of drinking water (DW) supply are required (WHO, 2017; 2022). In fact, one of the Sustainable Development Goals (SDG) is precisely to "Ensure the availability and sustainable management of water and sanitation for all" - SDG number 6 (UN, n.d.). Thus, securing microbial safety is indispensable to prevent contamination or reduce it to levels not harmful (WHO, 2022).

There are several ways from which microbial safety can be assured. One of the most common and used in many countries, including Portugal (Águas de Portugal, 2015), is using reactive chemical agents such as chlorine. This approach has been used since the beginning of the twentieth century (Bitton, 2014). However, in the

Netherlands, chlorine is not used at all (Smeets et al., 2009). Since chlorination has several limitations and is associated with the formation of chemical by-products that may be carcinogenic (Bitton, 2014; Smeets et al., 2009; WHO, 2022), the Dutch opt for a different strategy.

1.1.2 The Dutch Approach

Since 2005, chlorine disinfection has not been used in the Netherlands (Smeets et al., 2009). Alternatively, the Dutch prefer to use microbiologically safe groundwater for DW production as their primary water source. In fact, about 64% of its production is extracted from groundwater and 35% from surface water (rivers and lakes) (Ons Water, n.d.), as shown in Figure 1.1.

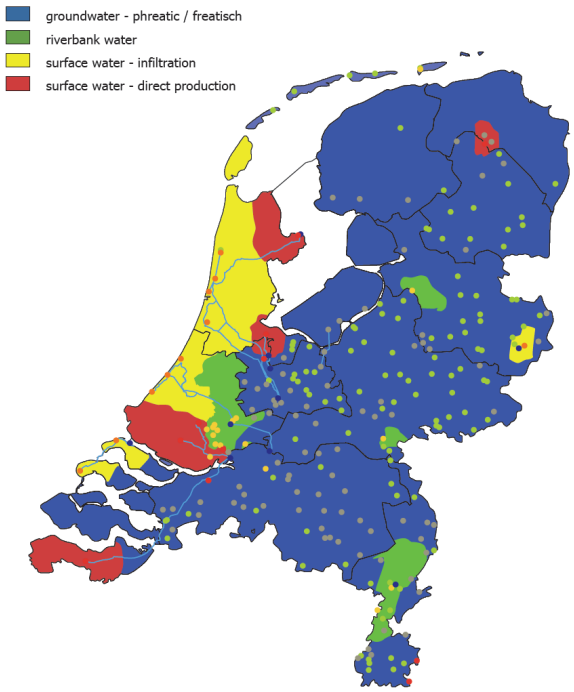

Figure 1.1: Drinking water production sources in the Netherlands. Retrieved from (Smeets et al., 2009).

Nonetheless, groundwater needs to be submitted to treatment since it contains inorganic compounds, such as iron, manganese, and ammonium, that can lead to unwanted microbial growth in the distribution system (de Vet et al., 2011). Therefore, the Dutch approach is to prevent that potential growth by starvation, i.e., to eliminate the microbial substrates of the water instead of suppressing its regrowth with a disinfectant residual (Smeets et al., 2009). As a result, DW is not only biostable but also has an improved taste and odour (Smeets et al., 2009).

To this end, the groundwater treatment in the Netherlands comprises the elimination of its main macro components - methane, carbon dioxide, iron, ammonium, and manganese. The withdrawal of the first two is achieved through aeration that will enable not only the gas exchange but also the oxygenation of water, essential to the oxidation of the remaining inorganic compounds (de Vet et al., 2010).

In contrast, to ensure the oxidation of the latter, Dutch Water Treatment Plants (WTP) use submerged rapid sand filters (Vries et al., 2021), further explained in Section 2.1. A scheme of a conventional groundwater treatment system with aeration and rapid sand filtration (RSF) phases are shown in Figure 1.2.

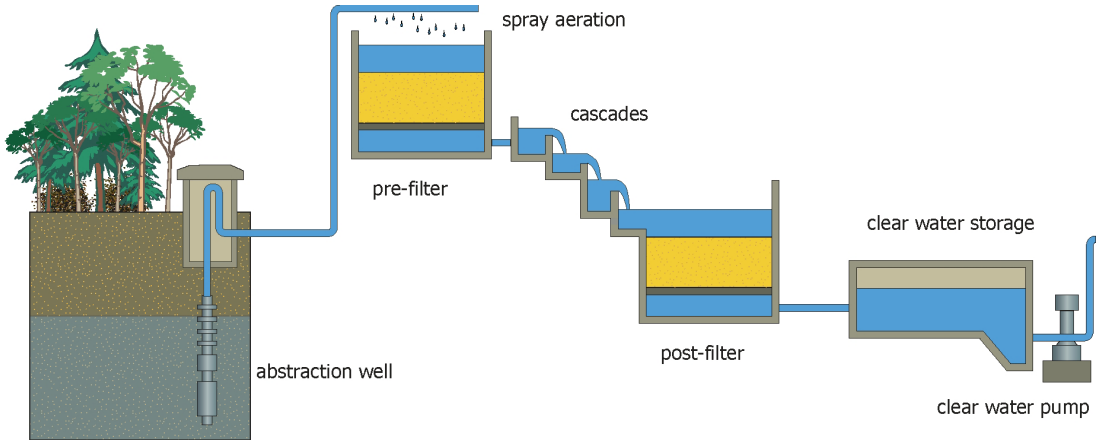

Figure 1.2: Schematic representation of a conventional groundwater treatment system. Retrieved from (de Vet et al., 2010).

Briefly, in a Dutch WTP, anaerobic groundwater is first abstracted and then, as previously stated, aerated to strip methane, carbon dioxide, and other volatile compounds from the water and ensure enough dissolved oxygen (DO) is present to oxidize iron, ammonia, and manganese. Then, it is filtered in RSF, where the sand grains function as adsorption surfaces onto which bacteria and oxides can adhere and promote the oxidation processes (de Moel et al., 2006). Thus, the RSF is considered to be more a "reactor" than a "filter" (de Moel et al., 2006).

As it will be deeply explained in Sections 2.2 and 2.3, iron and manganese oxidation can be both chemical and biological, but ammonia oxidation only occurs biologically. Equations 1.1 - 1.4 exclusively represent the biological oxidation reactions of the former elements, and Table 1.1 presents some of the microbial microorganisms that catalyze those reactions (de Vet et al., 2010).

$$Fe^{2+} + \frac{1}{4}O_2 + 1\frac{1}{2}H_2O \rightarrow FeOOH + 2H^+ \tag{1.1}$$

$$NH_4^+ + \frac{3}{2}O_2 \rightarrow NO_2^- + 2H^+ + H_2O \tag{1.2}$$

$$NO_2^- + \frac{1}{2}O_2 \rightarrow NO_3^- \tag{1.3}$$

$$2Mn^{2+} + \frac{1}{2}O_2 + 2H_2O \rightarrow Mn_2O_3 + 4H^+ \tag{1.4}$$

Although Rapid Sand Filtration has been practised for several years, and there has been an increasing number of publications in the last years, little is still known about the complexity of the microbial community and their role in RSF (Gülay et al., 2016).

1.2 Addressing Problem

Even though the studies comprising the diversity and distribution of microorganisms in RSF are scarce and have only been recently reported (Gülay et al., 2016), it is known that there is a relatively homogeneous vertical biomass distribution throughout the filter (Hammes et al., 2011).

Table 1.1: Oxidizing microorganisms of iron, ammonium and manganese for groundwater treatment (de Vet et al., 2010; Madigan et al., 2019).

Compound oxidation	**Microbial Microorganisms**
Iron	- Iron-oxidizing bacteria (*Gallionella ferruginea*, *Leptothrix ochracea*, *Sphaerotilus natans*, *Toxothrixt trichogenes*)
Ammonium	- Ammonia-oxidizing bacteria (*Nitrosomonas* spp. and *Nitrosospira* spp.) - Ammonia-oxidizing archae - "Comammox" bacteria (*Nitrospira* spp.)
Manganese	- Manganese-oxidizing bacteria (*Leptothrix* spp., *Metallogenium* spp., *Hyphomicrobium* spp., *Siderocapsa* spp., *Siderocystis* spp.)

Nevertheless, Environmental Biotechnology and Sanitary Engineering research groups from TU Delft have noticed that ammonia oxidation is not evenly distributed throughout the filter bed. In fact, even though there are ammonia-oxidizing microorganisms (bacteria, AOB, and archaea, AOA) all over the bed (de Vet, Dinkla, et al., 2009), this process occurs mainly at the bottom of the filter, when most of the iron has been oxidized. Moreover, it has also been noticed that ammonia oxidation occurs at the top of the filter when iron is not in the water (Tatari et al., 2013). Figure 1.3 presents data collected from different Drinking Water Treatment Plants (DWTP), where iron and ammonia concentrations were measured throughout the RSF at different stages, to help further understand the addressing problem.

In figures 1.3a and 1.3b, it is clear that ammonia removal barely occurs in the first filter. Instead, it only starts to oxidize in the second filter, where iron is no longer present.

In Figures 1.3c and 1.3d, ammonia concentration remains practically constant in the first section of the filter. Its complete removal only happens between the second and third sampling points once iron concentrations are below 1 mg/L.

In Figure 1.3e, although most of the ammonia removal occurs between the first and second sampling points, when iron is still being oxidized, its concentration is lower than in the previous examples (only 0.2 mg/L).

Based on all these full-scale DWTP pieces of information and knowledge from the literature (de Vet, Rietveld, et al., 2009), it is believed that iron might somehow interfere with the ammonia oxidation process.

Thus, two hypotheses were formulated to explain this phenomenon.

The first relates to the iron oxides (FeOx) that coat the sand grains. FeOx are formed upon the iron oxidation process and are then adsorbed onto the surface of the sand grains (explained in more detail in Section 2.2). Consequently, these compounds might, in some way, inhibit the ammonia-oxidizing microorganisms (AOM) from oxidizing the ammonia. The other hypothesis relies on the formation of radical oxygen species (ROS) during iron oxidation. It is known that when iron(II) reacts with molecular oxygen, it generates ROS as by-products (King et al., 1995). Since this species can be toxic to certain microorganisms, including AOM (Tolar et al., 2016), it can hinder the ammonia oxidation process. A more detailed description of these mechanisms is covered in Section 2.4.

Therefore, this work aims to understand what phenomenon may be inhibiting the ammonia oxidation process.

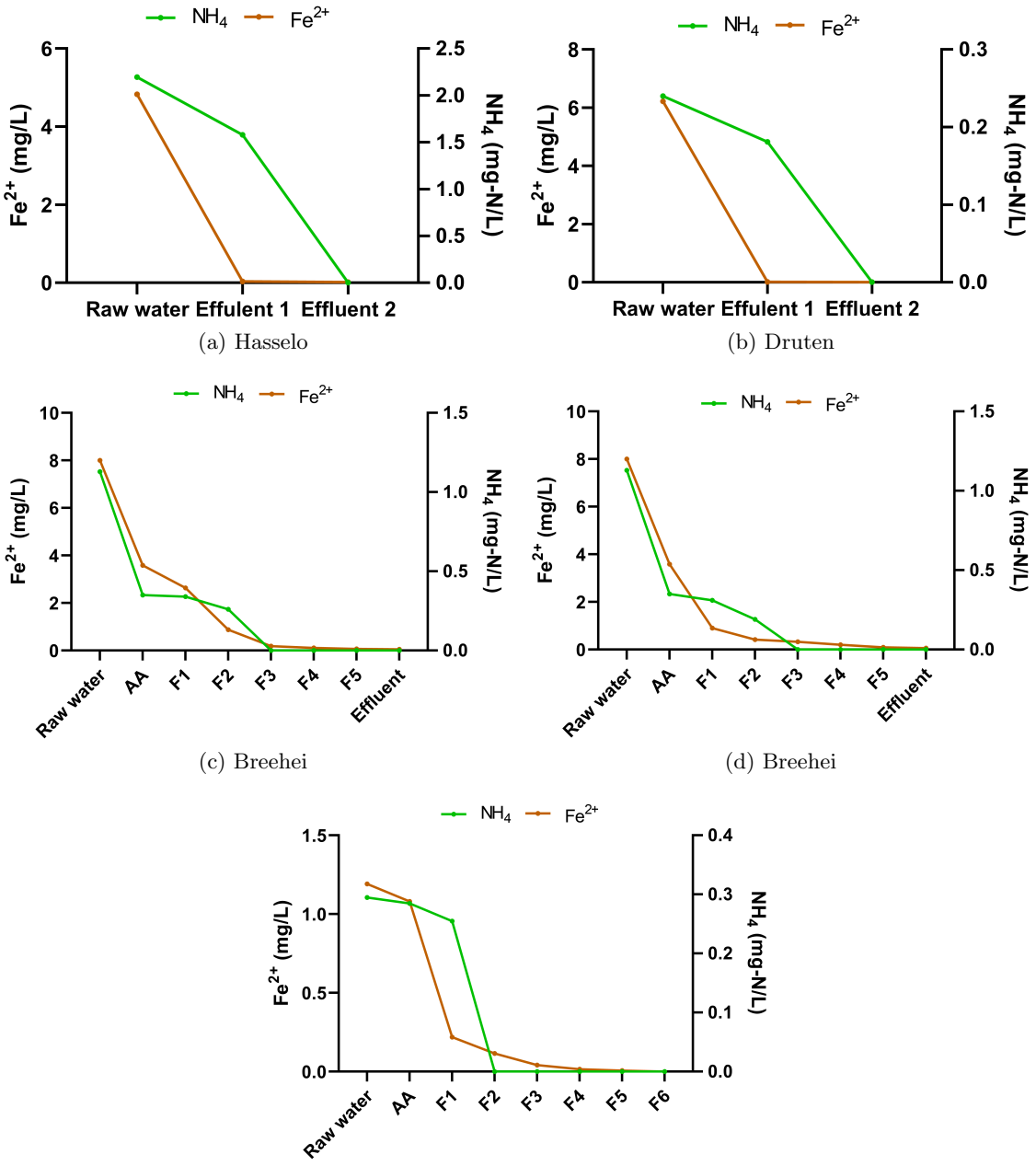

(a) Hasselo

(b) Druten

(c) Breehei

(d) Breehei

(e) Culemborg

Figure 1.3: Evolution of ammonia and iron(II) concentrations at different stages of the production of Drinking Water in five different Drinking Water Treatment Plants in the Netherlands - Hasselo (a), Druten (b), Breehei (c) and (d), and Culemborg (d). The samples were withdrawn before the aeration step (Raw Water), after the aeration step (AA) and at different filter heights (F1, F2, F3, F4, F5, and F6). In figures (a) and (b), only raw water and effluents of two consecutive filters were measured.

Research Question

Which are the underlying mechanisms behind the iron-caused ammonia oxidation inhibition in Rapid Sand Filtration?

Is the oxidation reaction *per se*, i.e., the formation of reactive oxygen species? Or the resulting product, i.e., the iron oxide-coating on the sand grains?

To test the first hypothesis, three lab-scale Rapid Sand Filter columns were custom-made to test two different filter media - virgin quartz sand and FeOx-coated sand.

If the iron oxides coating the sand are hindering ammonia oxidation, it will be possible to observe differences in the microbial colonization of the columns, as well as their removal profiles. Otherwise, iron oxides are not responsible for ammonia oxidation inhibition if no significant difference is observed between these two media.

To tackle the second hypothesis, ammonia oxidation rates will be monitored using sand grains containing ammonia oxidation activity and ROS quenchers in batch tests. In this case, if the addition of those scavengers does not neutralize ammonia oxidation inhibition, ROS may not be the primary cause.

Lastly, Fe^{2+} will be added to one of the lab-scale columns for a short period, and the ammonia oxidation profile will be monitored to understand how fast the system recovers.

1.3 Outline of the Thesis

To ease the comprehension of this Dissertation, the Master's student divided the document into six chapters:

- Chapter 1, Introduction, aims to give the reader the framework and motivation that led to the development of this work, briefly explaining how it was conducted.
- Chapter 2, Literature Review, seeks to provide a solid theoretical background that deeply enables the reader to understand the concepts behind the development of the work.
- Chapter 3, Materials and Methods, describes all the methodology used in the course of the laboratory and analytical work.
- Chapter 4, Results and Discussion, presents all the obtained results described in the previous Chapter, critically reviews the results and debates them based on the known literature.
- Chapter 5, Conclusions, intends to summarize the main conclusion after these five months of work and illustrate how it contributes to the progress of optimizing Rapid Sand Filtration.
- Chapter 6, Future Recommendations, provides additional ideas and experimental designs to test different theories that aim to understand the actual cause of the problem.

Additionally, all the necessary supplementary materials supporting the findings and leading to a more straightforward understanding are available in Appendixes A and B.

Chapter 2

Literature Review

2.1 Rapid Sand Filtration

Rapid Sand Filtration, as previously mentioned, is a method used to produce DW from groundwater. Contrarily to Slow Sand Filtration (SSF), RSF usually has higher flow rates (3-25 m/h) (Breda, 2019; Hammes et al., 2011). SSF, on the other hand, operates between 0.05 and 0.3 m/h (Breda, 2019; Hammes et al., 2011). Another significant distinction is that RSF is used after the aeration step to remove groundwater's major contaminants - iron, ammonia, and manganese. SSF, however, is typically placed at the end of the DWTP for disinfection purposes (Hammes et al., 2011).

Significant differences are also found regarding the microbial community and operational and structural parameters (Hammes et al., 2011). Nevertheless, since RSF is the sole method of this research, this section will focus on this technique.

Hence, RSF consists of a deep-bed filter (approximately 1 to 3.5 m in height) containing a coarse, porous material (Hammes et al., 2011). Traditionally, this filter bed is composed of quartz sand, although more recent practices use anthracite, calcium carbonate, or other granular media (Breda, 2019; Hammes et al., 2011; Michel et al., 2020).

This step in a DWTP may have one or several filtration units running in parallel, from which each unit can have one or two filters running in series (Breda, 2019).

Due to being employed in the first steps of the DW production, where iron is oxidized, RSF clogs relatively quickly and must be backwashed frequently (Hammes et al., 2011). Backwashing is necessary when operating RSF to restore their hydraulic retention function due to the inadvertent accumulation of precipitated oxides and other aggregates (Ramsay et al., 2021; Wang et al., 2021). This procedure usually involves washing the column in a reverse flow direction with water-only, air-only, or concurrent air+water, the latter considered the most aggressive backwashing procedure (Ramsay et al., 2021; Tekerlekopoulou et al., 2013). Thus, RSF should be gently washed so that the media's natural biofilm coating is not removed and the bed is not displaced from their original depth (Ramsay et al., 2021; Tekerlekopoulou et al., 2013). Backwash rates, frequency, and times are always adapted to each filter based on experience and performance (Tekerlekopoulou et al., 2013). Nonetheless, upwards water flows of 4-21 L/(m^2 s) are commonly used.

One disadvantage of RSF is the high start-up period (Breda, 2019; Etcheberry et al., 2022). However, this is where the success of the biofilter relies upon (Tekerlekopoulou et al., 2013). The natural start-up of a rapid sand filter usually takes about 2-3 months before it is complete (Y. Cai et al., 2015). Achieving complete

nitrification has been reported to take between 25 and 40 days, and complete manganese removal from 15 to 75 days (Etcheberry et al., 2022). When filter media consists of virgin sand, it may take more than a year for manganese to be entirely oxidized (Bruins et al., 2015). Thus, several start-up strategies have been developed to shorten the ripening time of these biofilters. Inoculation with backwash sludge from a well-established filter, use of old filter sand to withdraw some of the biomass, inoculation with nitrifying sludge, and mixing virgin with aged sand as filter media are some of the examples of these strategies (Bruins et al., 2015; Y. Cai et al., 2015; Qin et al., 2009; Štembal et al., 2004; Tekerlekopoulou et al., 2013; Wakelin et al., 2010).

2.2 Iron oxidation

As stated in Subsection 1.1.2, groundwater is the primary source of drinking water in The Netherlands. Since Fe^{2+} is one of its most common contaminants, its oxidation is assured by water oxygenation during the aeration phase. In this step, O_2 diffuses into the groundwater and facilitates the oxidation of iron(II) into iron(III)-hydroxides precipitates (Vries et al., 2021).

However, the aeration phase is insufficient to oxidize all Fe^{2+} from the water. Instead, its complete removal is only accomplished within the rapid sand filters. As such, it is possible to distinguish between these two phenomena. In the former, iron(III)-hydroxides precipitate directly from iron(II) and oxygen by a combination of oxidation and hydrolysis - called homogeneous or flocculent oxidation. In the latter, iron(III)-hydroxides precipitation mainly occurs after being preceded by adsorption of iron(II) onto existing surfaces, typically sand grains (van Beek et al., 2016; van Beek et al., 2012) - and it is then called heterogeneous or adsorptive oxidation.

Nevertheless, these two are not the only iron oxidation processes within the sand filters. There is also biological oxidation carried out by iron-oxidizing bacteria (IOB) attached to the filter media (van Beek et al., 2016; van Beek et al., 2012). In this case, the energy produced during the reaction is converted into the microorganisms, and the iron(III)-hydroxides are either precipitated internally or excreted into the extracellular polymeric substance (EPS) (van Beek et al., 2012).

Thus, there are three types of iron(II) oxidation mechanisms in RSF - homogeneous, heterogeneous, and biological, each competing with the other. To understand the conditions favourable for each process, Table 2.1 summarizes its overall reactions. Hence, pH, oxygen concentration, and iron(III)-hydroxides concentration play a crucial role in determining which iron oxidation process is favoured.

Table 2.1: Overall chemical reactions of homogeneous, heterogeneous, and biological iron(II) oxidation. Adapted from (van Beek et al., 2016; van Beek et al., 2012).

Iron oxidation	**Overall reaction**
Homogeneous	$Fe^{2+} + \frac{1}{4}O_2 + H_2O \rightarrow Fe(OH)_3 + 2H^+$
Heterogeneous	$S - HO^0 + Fe^{2+} + \frac{1}{4}O_2 + \frac{3}{2}H_2O \rightarrow S - OFe(III)(OH)_2^0 + 2H^+$
Biological	$Fe^{2+} + \frac{1}{4}O_2 + \frac{1}{2}H_2O \rightarrow Fe(OH)_3 + 2H^+ + FeOB - biomass$

van Beek et al. (2016) have studied the contribution of iron(II) oxidation in RSF and concluded that even though each process depends on temperature, chemical

composition, reaction rates, etc., it is possible to establish a pH-dependence relation (Figure 2.1). According to their study, heterogeneous oxidation is significant at low pH (6.5 - 7); between 6.5 and 7.7, biological oxidation is the dominant process; and, at higher pH, homogeneous oxidation prevails (van Beek et al., 2016). Since adsorptive oxidation requires a surface, heterogeneous oxidation is also preferred when Fe(III)-hydroxides concentration is high (van Beek et al., 2012).

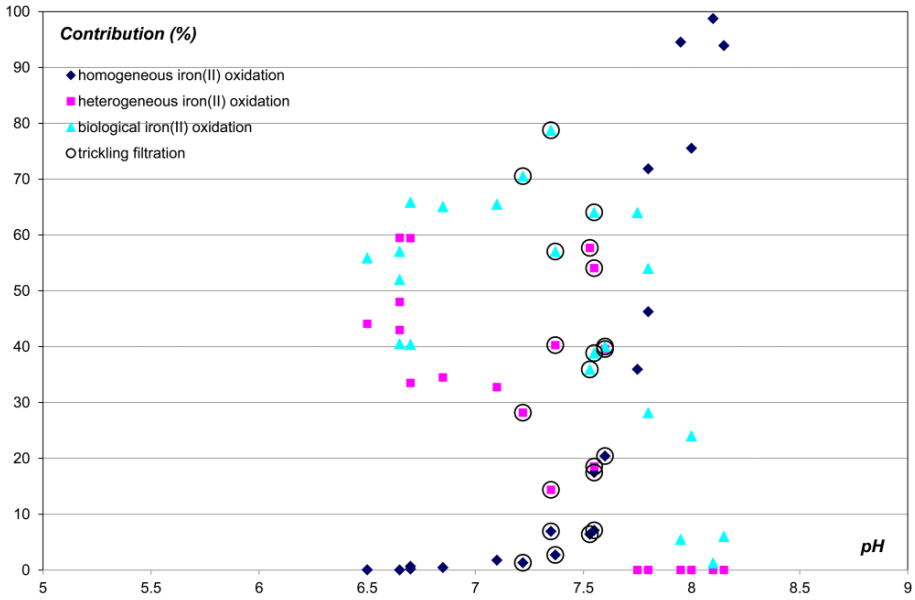

Figure 2.1: Contribution of the iron(II) oxidation processes to Rapid Sand Filtration as a function of pH. Retrieved from (van Beek et al., 2016).

Even though all the reactions from Table 2.1 oxidize Fe^{2+} into Fe^{3+}, their products and consequent effects are significantly different. Homogeneous oxidation is characterized by forming iron flocs, whereas heterogeneous oxidation causes the filter media to grow due to the adsorption of the iron(III)-hydroxides onto the sand grains (van Beek et al., 2016; van Beek et al., 2012). These iron oxides (FeOx) will then alter the physical-chemical properties of the media (Truesdail et al., 1998), which will consequently change its adsorption capacity (Mills et al., 1994). On the other hand, the iron oxidation reaction itself will form radical species such as the superoxide anion, hydrogen peroxide, or hydroxyl radical (Emmenegger et al., 1998; King et al., 1995; Rose et al., 2002) that can then react with other elements in the filter.

2.2.1 Iron Oxides

There are several types of iron oxides (mentioned in Table 2.2), divided into three categories: oxides, hydroxides, and oxide-hydroxides (Cornell et al., 2003). From these 16 oxides, goethite, lepidocrocite, and ferrihydrite are found in RSF systems (van Beek et al., 2012).

Ferrihydrite (HFO), a reddish-brown oxide, is the most abundant form of RSF. It is formed upon fast Fe^{2+} oxidation with O_2 and, with time (1-2 years), may transform into a more stable and better crystalline FeOx, goethite (Cornell et al., 2003; van Beek et al., 2012). However, lepidocrocite, an orange-coloured oxide, can also be formed to a lesser extent when a slower Fe^{2+} oxidation occurs (Cornell et al., 2003; van Beek et al., 2012).

Even though there are oxides containing iron in its divalent state (FeO, $Fe(OH)_2$, and Fe_3O_4), the aforementioned compounds are comprised of Fe^{3+} (Cornell et al., 2003). Hence, it is clear that in RSF, only Fe(III)-hydroxides are present coating the sand grains.

Table 2.2: Different types of iron oxides. Retrieved from (Cornell et al., 2003).

Oxide-hydroxides and hydroxides	**Oxides**
Goethite, $\alpha - FeOOH$	Hematite, $\alpha - Fe_2O_3$
Lepidocrocite, $\gamma - FeOOH$	Magnetite, $Fe_3O_4(Fe^{II}Fe_2^{III}O_4)$
Akaganéite, $\beta - FeOOH$	Maghemite, $\gamma - Fe_2O_3$
Schwertmannite, $Fe_{16}O_{16}(OH)_y(SO_4)_z \cdot nH_2O$	$\beta - Fe_2O_3$
$\delta - FeOOH$	$\epsilon - Fe_2O_3$
Feroxyhyte, $\gamma' - FeOOH$	Wüstite, FeO
High pressure $FeOOH$	
Ferrihydrite, $Fe_5HO_8 \cdot 4H_2O$	
Bernalite, $Fe(OH)_3$	
$Fe(OH)_2$	
Green Rusts, $Fe_x^{III}Fe_y^{II}(OH)_{3x+2y-z}(A^-)_z; A^- = Cl^-; \frac{1}{2}SO_4^{2-}$	

Iron oxides have many properties, of which their high adsorption capacity, porosity, surface area and pH-dependent surface charge stand out (Cornell et al., 2003).

Compared to virgin sand as a filter media, iron oxides-coated sand has a much higher porosity, adsorption capacity and surface area (Sharma et al., 1999; Sharma et al., 2002). Moreover, it also possesses a higher surface charge than quartz sand due to its more elevated point of zero charge (pzc) (Schwertmann et al., 1982).

The pzc is the pH value at which the net adsorption of ions onto the oxides is zero. It can also be referred to as isoelectric point (iep - the pH at which the net surface charge is zero) if there is no specific adsorption under discussion (Cornell et al., 2003).

Thus, the pzc depends on the functional groups on the surface of the oxides. At pH's values < pzc, $FeOH_2^+$ prevail over $FeOH^-$ groups, meaning that the crystal will have an overall positive net charge and adsorb negative particles (Cornell et al., 2003).

Since the composition of HFO is variable, so it is its pzc. According to Cornell et al.; Schwertmann et al., ferrihydrite's pzc can vary between 5.3 and 7.9.

2.2.2 Reactive Oxygen Species

Iron(II) reaction with oxygen usually yields iron(III)-hydroxides, as previously mentioned. However, in aqueous solution, it can also produce reactive oxygen species (ROS), particularly the superoxide anion, $O_2^{\bullet-}$, and hydrogen peroxide, H_2O_2, - reactions 2.1 and 2.2 (Emmenegger et al., 1998; King et al., 1995).

$$Fe^{2+} + O_2 \rightarrow Fe^{3+} + O_2^{\bullet-} \tag{2.1}$$

$$Fe^{2+} + O_2^{\bullet -} + 2H^+ \rightarrow Fe^{3+} + H_2O_2 \tag{2.2}$$

Hydrogen peroxide is a well-known ROS with a lifetime of 2-4 hours and a reduction potential of E^0=1.76V in an acidic solution and E^0=0.88V in an alkaline medium (Wilson et al., 2000; Zhou et al., 2018). This radical can then react with Fe^{2+} itself and form a different type of ROS, $HO^{\bullet}$, through the "classical" Fenton reaction (equation 2.3). $HO^{\bullet}$, on the other hand, is the second most potent ROS known (E^0=2.8V) (Zhou et al., 2018), but its lifetime is estimated to be around 10^{-9} seconds, meaning it has to be generated *in situ* to non-selectively oxidize organic compounds (He et al., 2016; Zhou et al., 2018).

$$Fe^{2+} + H_2O_2 \rightarrow Fe^{3+} + HO^{\bullet} + HO^- \tag{2.3}$$

These two ROS can then trigger chain reactions and interact with other species, forming more ROS and neutralizing themselves in a cyclic pathway - equations 2.4-2.9 (Ameta et al., 2018; Rose et al., 2002; Zhou et al., 2018).

$$HO^{\bullet} + H_2O_2 \rightarrow HO_2^{\bullet} + H_2O \tag{2.4}$$

$$Fe^{2+} + HO^{\bullet} \rightarrow Fe^{3+} + HO^- \tag{2.5}$$

$$Fe^{3+} + HO_2^{\bullet} \rightarrow Fe^{2+} + O_2 + H^+ \tag{2.6}$$

$$HO_2^{\bullet} \rightleftarrows H^+ + O_2^{\bullet -} \tag{2.7}$$

$$FeOOH^{2+} \rightarrow Fe^{2+} + HO^{\bullet} \tag{2.8}$$

$$HO^{\bullet} + HO^{\bullet} \rightarrow H_2O_2 \tag{2.9}$$

However, there is more to Fenton than the "classical" homogeneous reaction. Nowadays, Fenton can be divided into Fenton and Fenton-like reactions, with the latter being addressed when other metals, such as Fe^{3+}, Co^{2+}, Cu^{2+}, or Mn^{2+}, are used (Ameta et al., 2018; Pereira et al., 2012). Besides, it can still be classified into homogeneous, heterogeneous, and Photo-Fenton (He et al., 2016).

Homogenous Fenton reaction, as previously mentioned, occurs when H_2O_2 oxidizes ferrous ions (equation 2.3), whereas the heterogeneous reaction develops with iron in a solid matrix, like iron-(hydro)oxides (Pereira et al., 2012). Fenton-like reaction (equation 2.10) can also occur depending on the oxidation state of the iron(hydro)oxides (Ameta et al., 2018; Pereira et al., 2012), as illustrated in Figure 2.2.

$$Fe^{3+} + H_2O_2 \rightarrow FeOOH^{2+} + H^+ \tag{2.10}$$

$$FeOOH^{2+} \rightarrow Fe^{2+} + HO^{\bullet} \tag{2.11}$$

$$Fe^{3+} + HO_2^{\bullet} \rightarrow Fe^{2+} + O_2 + H^+ \tag{2.12}$$

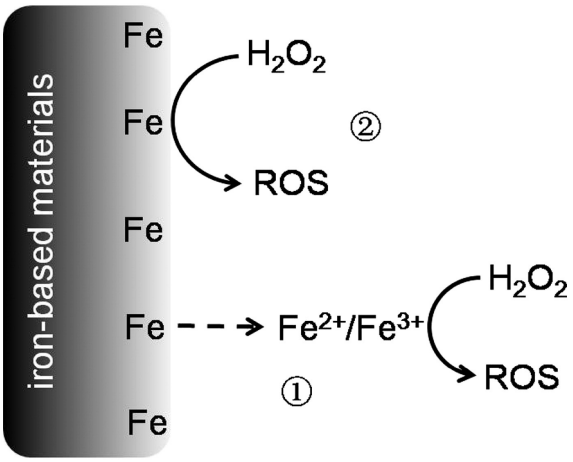

Figure 2.2: Schematic representation of interfacial mechanisms of Fenton systems: 1) homogeneous Fenton induced by surface leached-iron and 2) heterogeneous Fenton and Fenton-like catalysis. Retrieved from (He et al., 2016).

Nevertheless, it is essential to understand that the homogeneous Fenton reaction has an optimal pH of 2.8-3.0 (Pereira et al., 2012; Zhou et al., 2018), meaning that the formation of $HO^{\bullet}$ in RSF systems might be limited to the in situ pH of the reaction.

On the other hand, heterogeneous and/or Fenton-like reactions do not have the same pH limitation (Pham, 2012, Pereira et al., 2012). Although these reactions are slower, relatively inefficient and usually form $HO_2^{\bullet}$, which has a lower oxidation power (E^0=1.70V) (Zhou et al., 2018), $HO^{\bullet}$ formation can also occur through reaction 2.12 (Pereira et al., 2012).

Moreover, Fenton can also occur through a newly suggested reaction (equation 2.13), which explains the detection of ferryl (Fe^{4+}) ions, capable of oxidizing organic molecules by electron transfer. However, more research is needed, especially to understand how variables like pH affect the reaction (Zhou et al., 2018).

$$Fe^{2+} + H_2O_2 \rightarrow [Fe(OH)_2]^{2+} \rightarrow Fe^{3+} + HO^{\bullet} + HO^{-} \tag{2.13}$$

Thus, there are many pathways from which ROS can be formed upon iron oxidation in aquatic ecosystems (Morris et al., 2022). Even though Fenton reactions are incredibly complex yet not fully understood, it is vital to assess how their presence can affect the RSF system and, ultimately, the ammonia oxidation process.

2.3 Ammonia oxidation

2.3.1 The Nitrogen Cycle

Nitrogen is the fourth most abundant element in cellular biomass, essential for the biosynthesis of proteins and nucleic acids (Kuypers et al., 2018; Stein et al., 2016). Despite comprising most of Earth's atmosphere, dinitrogen gas (N_2) is not accessible as a nitrogen source for most living organisms (Kuypers et al., 2018; Stein et al., 2016). Instead, it first has to be converted to ammonia through nitrogen fixation; only then can it be assimilated into cellular life (Kuypers et al., 2018; Stein et al., 2016).

Traditionally, the Nitrogen cycle has been divided into three pathways - N_2 fixation, nitrification, and denitrification (Stein et al., 2016). Currently, it can be divided into seven major metabolic conversions, illustrated in Figure 2.3. Through these conversions, nitrogen compounds range from -3 to +5 oxidation states using 14 redox reactions (Kuypers et al., 2018).

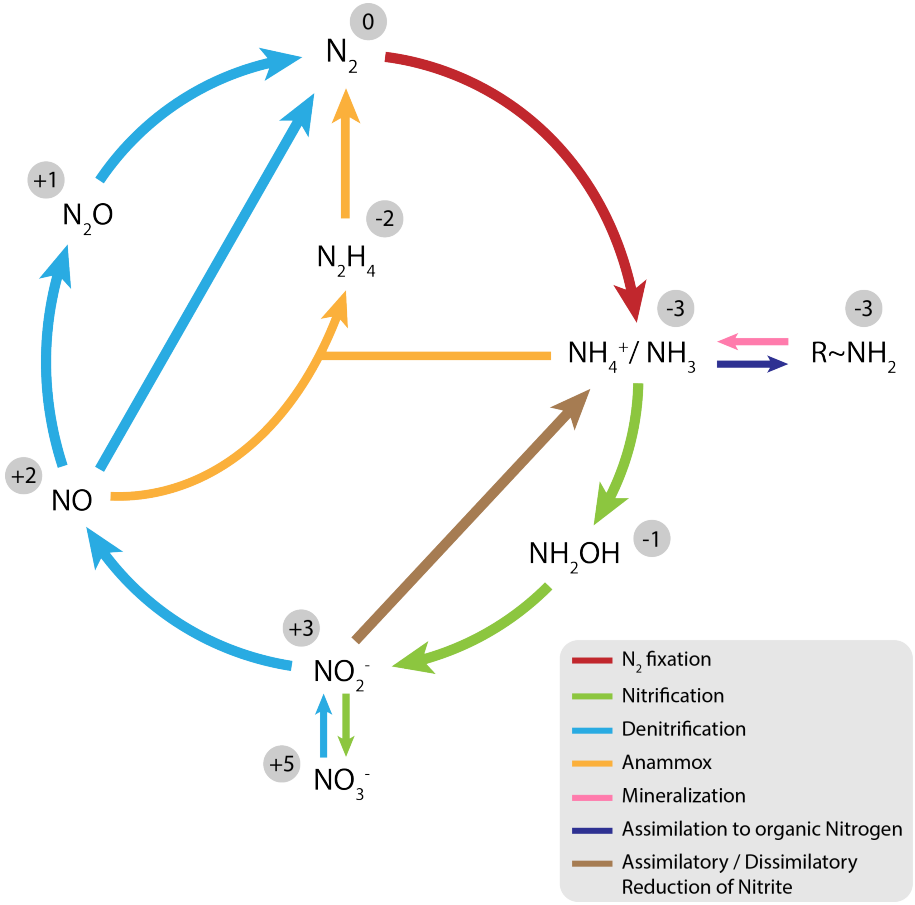

Figure 2.3: The Nitrogen Cycle, with each pathway represented in different colors. The oxidation state of nitrogen in each of the intermediates is outlined inside the grey circles. Based on Stein et al., 2016

Before the invention of the Haber-Bosch process in 1909, Nitrogen fixation was limited to microorganisms that encoded nitrogenase metalloenzyme (Kuypers et al., 2018; Stein et al., 2016). Nowadays, however, most fertilizers rely on this method, leading to excess nitrogen fixation over denitrification and, consequently, an unbalanced cycle (Bender, 2012).

Even though understanding the whole cycle is crucial for Environmental Biotechnology, only nitrification (ammonium oxidation to nitrate) is present in RSF systems. Thus, this section will focus on that part of the cycle.

Nitrification is a 2-step process, where ammonia is first oxidized to nitrite and subsequently to nitrate (van Kessel et al., 2015). Equations 2.14 and 2.15 represent the first step of nitrification - ammonia oxidation - whereas equation 2.16 describes the second step - nitrite oxidation (Zannoni, 2004).

Until the discovery of the *Nitrospira* bacteria in 2015, these oxidations were believed to be performed by two different types of microorganisms - ammonia-oxidizing bacteria or archaea and nitrite-oxidizing bacteria (van Kessel et al., 2015). However, it is now known that *Nitrospira* bacteria contain the genetic information to

catalyze both nitrification steps in one living organism, thus being able to perform the complete ammonia oxidation, "Comammox" (Daims et al., 2015).

Moreover, in 2017, Caranto et al. discovered that bacterial reaction 2.15 does not occur as globally accepted. Hydroxylamine oxidoreductase (HAO) produces nitrous oxide (NO) - rather than NO_2^- -, which is then further oxidized to the final product by a still unknown enzyme. According to Stein, since HAO differs between bacteria and archaea, the pathway of the latter is still to be discovered (Stein, 2019).

$$NH_3 + O_2 + 2e^- + 2H^+ \rightarrow NH_2OH + H_2O \tag{2.14}$$

$$2NH_2OH + H_2O \rightarrow NO_2^- + 4e^- + 5H^+ \tag{2.15}$$

$$NO_2^- + H_2O \rightarrow NO_3^- + 2H^+ + 2e^- \tag{2.16}$$

It is thus clear that the understanding of nitrification is still far from complete. Nonetheless, it is of utmost importance to comprehend the metabolism of ammonia-oxidizing microorganisms to achieve progress.

2.3.2 Nitrifiers

Nitrifiers are, as the name suggests, microorganisms able to perform nitrification. It thus comprises ammonia and nitrite-oxidizing microorganisms.

Ammonia Oxidizers

There are two major groups of ammonia-oxidizing microorganisms (AOM) - bacteria (AOB) and archaea (AOA). Both are chemolithoautotrophs, which means that they derive their energy from the oxidation of ammonia to nitrite, and meet their carbon requirements from CO_2 or carbonates (Robertson et al., 2015; Sayavedra-Soto et al., 2011; Stein et al., 2016). Although obligate aerobes, these microorganisms can undergo anaerobic and anoxic conditions, meaning the lack of oxygen is not lethal (Brown et al., 2013). Additionally, there are heterotrophic and methanotrophic microorganisms capable of oxidizing ammonia to nitrite. However, this reaction is not linked to cellular growth (Robertson et al., 2015; Stein et al., 2016).

Due to the last decade's technological development, 16S rRNA gene sequence analysis enabled a better classification of AOM. Thus, it is now known that AOB are classified as Proteobacteria (Betaproteobacteria and Gammaproteobacteria) and AOA as Thaumarchacota. Commammox bacteria, on the other hand, are a part of the Nitrospirae phylum. (Robertson et al., 2015; Stein, 2019).

Equations 2.14 and 2.15 represent ammonia oxidation to nitrite. The former is catalyzed by ammonia monooxygenase (AMO), whereas the latter is catalyzed by hydroxylamine oxidoreductase (HAO) (Kuypers et al., 2018; Stein, 2019). However, accounting for microbial growth, i.e., carbon uptake, and assuming a biomass yield of 0.2 mg biomass per mg of oxidized ammonia, the stoichiometry of both reactions is (Zhang et al., 2009):

$$\begin{aligned} NH_4^+ + 1.9\,O_2 + 0.069\,CO_2 + 0.0172\,HCO_3^- \\ \rightarrow 0.0172\,C_5H_7O_2N + 0.983\,NO_2^- + 0.966\,H_2O + 1.97\,H^+ \end{aligned} \tag{2.17}$$

Nitrite Oxidizers Oxidizers

Nitrite oxidation to nitrate is only performed by nitrite-oxidizing bacteria (NOB). These microorganisms, contrarily to AOB, belong to several classes of Proteobacteria (Alphaproteobacteria, Betaproteobacteria, and Gammaproteobacteria), Chloroflexi, Nitrispinae and Nitrospirae phyla (Kuypers et al., 2018; Stein et al., 2016). They are also chemolithoautotrophs, which means that they use nitrite as an energy source and CO_2 or carbonate as their carbon source (Robertson et al., 2015; Stein et al., 2016).

Equation 2.16 represents the oxidation reaction of nitrite, catalyzed by nitrite oxidoreductase (NXR) (Kuypers et al., 2018). However, accounting for microbial growth, and considering a biomass yield of 0.1 mg per mg of oxidized nitrite, the stoichiometry of the reaction is (Zhang et al., 2009):

$$NO_2^- + 0.00875\,NH_4^+ + 0.035\,CO_2 + 0.00875\,HCO_3^- + 0.456\,O_2 + 0.00875\,H_2O \rightarrow 0.00875\,C_5H_7O_2N + NO_3^- \quad (2.18)$$

Limiting Factors

Nitrifiers are fragile microorganisms with a slow growth rate (between 3 to 6 days in the activated sludge process) since only 80% of the energy produced during nitrification is used to fix carbon into biomass (Gerardi, 2016b; Robertson et al., 2015). Thus, it is of utmost importance to consider the factors that may interfere with nitrification and nitrifiers' growth (Gerardi, 2016a).

The most significant factors mentioned in this section are: temperature, alkalinity, pH, dissolved oxygen (DO) concentrations, and orthophosphate concentrations.

The desirable temperature range for nitrification is between 20 and 25^{o}C. At 15^{o}C, 50% of the nitrification rate is lost; at 10^{o}C, the loss increases to 80%; and, below 8^{o}C, nitrification stops (Gerardi, 2016a).

Alkalinity is another crucial aspect. Because nitrifiers are autotrophs, bicarbonate (HCO_3^-) and carbonate (CO_3^{2-}) are their preferred carbon sources. Thus, for each mg of oxidized NH_4-N, 8.62 mg of HCO_3^- (14 mg/L $CaCO_3$) are required (Zhang et al., 2009).

If alkalinity is not enough, a change in pH can occur rapidly, which may be critical for the enzymatic structure and activity (Gerardi, 2016a). The optimum pH for nitrification ranges from 7.2 to 7.4, even though nitrifiers tolerate pH values between 6.5 to 8.0. However, damage to enzymes occurs below 6.5 or above 8.0; consequently, nitrification is inhibited (Gerardi, 2016a).

Nitrifying bacteria consume approximately 4.33 mg O_2 per mg of NH_4^+ oxidized to NO_3^- (Zhang et al., 2009). Depending on the culture and mass transfer conditions, nitrifiers grow best at concentrations between 2 and 3 mg O2/L; however, higher concentrations may also promote nitrification (Gerardi, 2016a; Zhang et al., 2009). Whilst AOB are less sensitive to low DO values, NOB may be hindered by it, resulting in nitrite accumulation in the system Gerardi, 2016a. Ammonia oxidizers can use nitrite or nitrate as an alternative electron acceptor when oxygen is low, enabling them to survive under low DO concentrations. Nonetheless, this process is not favourable enough to support cell growth (Zhang et al., 2009).

Lastly, phosphate is also an essential factor to consider. Usually, a concentration above 0.5 mg/L of phosphorous is required for nitrifying bacteria's growth (Gerardi, 2016a), although some authors recommend a minimum range between 3 and 20 µg-P/L (Zhang et al., 2009).

2.4 Possible interactions between species

2.4.1 Iron oxides and ammonia-oxidizing microorganisms

As mentioned earlier, the formation of iron oxide coating due to heterogeneous iron oxidation can modify the physical-chemical properties of the filter media (Truesdail et al., 1998).

In this case, the filter media consists of sand grains with a strong negative superficial charge (Mills et al., 1994; Truesdail et al., 1998). Since RSF is also a biological process, bacterial cells must be able to colonize the sand. However, bacteria have a negatively charged surface due to the predominance of anionic groups within the cell wall (Mills et al., 1994; Truesdail et al., 1998), consequently making colonization of virgin sand a slow process.

Nonetheless, previous studies have shown that the positively charged surface of iron oxides can ease bacterial adhesion onto the media (Mills et al., 1994; Truesdail et al., 1998). Moreover, studies from Sharma et al. showed that coated sand had a higher porosity and specific surface area, thus enhancing not only bacterial but also iron(II) adsorption (Sharma et al., 1999; Sharma et al., 2002). On top of that, FeOx coating onto the sand can also impact the microbial activity in RSF. Gülay et al. showed that the ammonia removal rate also increased with the amount of mineral coating (Gülay et al., 2014).

Therefore, it is expected that the presence of iron oxides covering the sand grains of RSF media can ease microbial adhesion and activity.

Nevertheless, it is known that nitrifiers are adapted to grow at iron concentrations as low as 0.2 µM (Sayavedra-Soto et al., 2011), meaning there is a chance that growth in a FeOx-coated grain might be toxic for them.

2.4.2 ROS and ammonia-oxidizing microorganisms

It is well known that ROS molecules are highly reactive and cause damage to living organisms (Vatansever et al., 2013). Thus, one probable hypothesis is that ROS formation upon iron oxidation harms ammonia-oxidizing bacteria and hinders the ammonia oxidation process.

Under aerobic conditions, as nitrification occurs, bacteria are more likely to experience oxidative stress and ROS production (Vatansever et al., 2013). These molecules can react with several cellular components, such as proteins, lipids, and nucleic acids, damaging them and compromising their function, e.g., enzymatic (Vatansever et al., 2013).

However, microorganisms can produce enzymes to neutralize these ROS, such as catalase, peroxidase, and superoxide dismutase (SOD) (Madigan et al., 2019; Vatansever et al., 2013).

Catalase breaks H_2O_2 into H_2O and O_2 through reaction 2.19; peroxidase also neutralizes H_2O_2 through a different mechanism (equation 2.20); and SOD dismutases $O_2^{\bullet-}$ into H_2O_2 and O_2 (reaction 2.21) (Madigan et al., 2019; Vatansever et al., 2013).

$$2\,H_2O_2 \rightarrow 2\,H_2O + O_2 \tag{2.19}$$

$$2\,H_2O_2 + NADH + H^+ \rightarrow 2\,H_2O + NAD^+ \tag{2.20}$$

$$2\,O_2^{\bullet -} + 2\,H^+ \rightarrow 2\,H_2O_2 + O_2 \tag{2.21}$$

Wood et al. (2001) found that different AOB strains possess activity for catalase and SOD, even though regulation and isoenzymes differ between strains. Kim et al. (2016), on the other hand, discovered that extracellular a-keto acids were fundamental to detoxifying ROS from certain AOA strains and that, in their absence, ROS would inhibit microbial growth.

Furthermore, it is essential to understand that not even these quenchers can prevent cellular damage above specific limiting concentrations. For instance, Tolar et al. found that concentrations of H_2O_2 above 10 nM were toxic to certain AOA strains but tolerable to others (Tolar et al., 2016).

Thus, it is of utmost importance to study if ROS production in RSF systems through Fenton or Fenton-like reactions is lethal to the existing nitrifier community.

Chapter 3

Materials and Methods

3.1 Columns Start-up

Lab-scale rapid sand filter columns were custom-made (Lenntech B.V., The Netherlands) according to the dimensions on Figure A.1 of Appendix A.1.

Sand samples were collected from *Vitens'* Drinking Water Treatment Plant in Hammerflier, The Netherlands.

Main pump (Masterflex, Germany), secondary pumps (Watson-Marlow B.V., The Netherlands), DO and pH probes (Mettler Toledo, USA), Bio Controller ADI 1030 (Gemini B.V., The Netherlands), tubing (Masterflex, Germany; Tygon, Saint-Gobain, France), connectors, chemical compounds (Sigma-Aldrich, USA; Merck, Germany), glassware, and disposable material were provided by TU Delft.

The filter media of the columns consisted of iron oxide (FeOx)-coated sand without ammonia oxidation activity (Figure A.2a) and virgin quartz sand with a high silica content (Figure A.2b) from Aqua-Techniek B.V., The Netherlands. The three columns were filled with 240 g of virgin sand, 120 g of virgin sand + 110 g of FeOx-coated sand, and 190 g of FeOx-coated sand so that the media volume was the same in all of them.

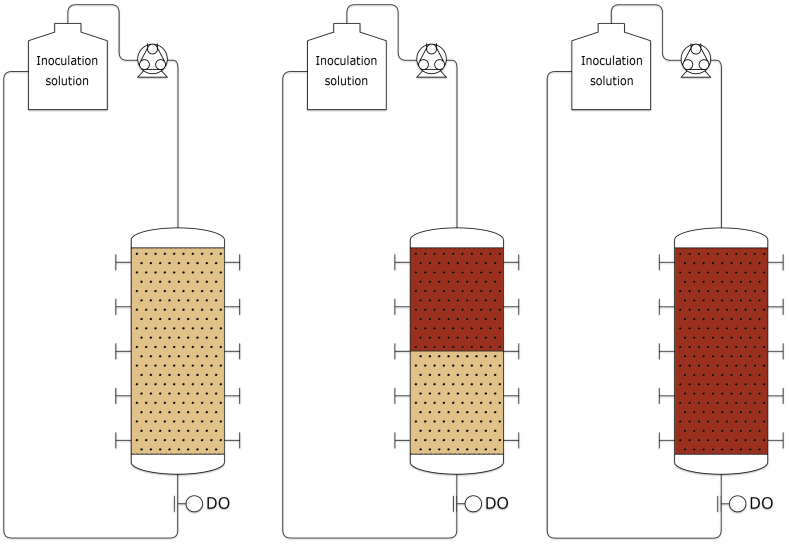

Figure 3.1: Schematic representation of start-up strategy in the columns. Virgin quartz sand column on the left, FeOx-virgin sand column in the middle, and FeOx-coated sand column on the right.

The lack of ammonia oxidation activity was tested as described in Section A.2.

As mentioned in Section 2.1, a rapid sand filter's natural start-up usually takes several months. Thus, a start-up strategy was implemented due to this MSc Thesis's limited time.

Sand samples containing ammonia-oxidizing microorganisms were used to obtain an inoculation solution. The protocol was adapted from Wakelin et al. (2010). and consisted of vortexing 0.5 g of sand with 1 mL of tap water for 1.5 minutes. The sand grains were filtered afterwards, and the resulting solutions were re-circulated for 25 days in a close circuit at a superficial velocity of 1.5 m/h, as illustrated in Figure 3.1. Ammonia to a final concentration of 10 mg-N/L was added whenever necessary.

On the 10th and 20th days, activated sludge from a Wastewater Treatment Plant (WWTP) in Amsterdam was added to the columns to boost the inoculation procedure. Protocol from Y. Cai et al. (2015) was adapted to the volume of the columns (250 mL) and the VSS content of the sludge (4.6 g/L).

3.2 Columns Tests

After the inoculation procedure, the columns were switched from a closed circuit to a continuous mode system, as shown in Figure 3.2. A mixture of tap water with the desired growth medium was kept flowing downwards at superficial velocity of 1.5 m/h and a pH of 7.7 - 7.9. Effluent's pH ranged from 6.9 to 7.3.

Column maintenance was performed daily, and a mild backwash with an average flow rate of 13.6 L/h for 9 min was performed daily when iron(II) was supplemented in the influent.

Figure 3.2: Lab-scale rapid sand filtration columns used throughout this Thesis.

3.2.1 Evaluating the role of FeOx-coated sand on the process of ammonia oxidation

Virgin sand as a filter media was compared to FeOx-coated sand to study the influence of iron oxides upon ammonia oxidation. To prevent interference of ROS in this condition, no iron(II) was added to the system.

The growth medium was thereby adapted from Soler-Jofra et al. (2018) and composed of 380 mg/L NH_4Cl (100 mg/L NH_4-N), 87 mg/L K_2HPO_4, and 3 mL/L of Trace Elements solution (detailed composition in Section A.3), and added to the columns at a flow rate of 14.7 mL/h.

The final ammonium content in the influent of the columns was thus 2.0 mg/L NH_4-N to mimic the natural ammonia concentration of groundwater (de Moel et al., 2006).

Water samples were taken thrice per week (as detailed in Section A.4) at four different sampling points in each column for 4 weeks.

3.2.2 Evaluating the effect of iron(II) addition into the system

A solution of 1.78 g/L $FeCl_2$ (500 mg/L of Fe^{2+}) was added to the column composed of half virgin sand - half FeOx coated sand at a flow rate of 4.4 mL/h to a final iron(II) content in the column of 3.0 mg/L of Fe^{2+}. Although iron (II) concentration in groundwater is usually around 8.8 mg/L (de Moel et al., 2006), after the aeration step, i.e., when entering the RSF, iron content usually does not exceed 4 mg/L (as seen in Subsection 1.2).

Ammonia and the remaining growth medium with tap water were continuously added to the column, as previously described.

The addition of iron lasted one day. Afterwards, the column was rerun under the previous conditions, and the column's recovery profile was analyzed in the following 3 weeks.

Water samples were taken twice weekly (as detailed in Section A.4) at five different sampling points.

3.3 Batch Tests

3.3.1 Evaluation of iron(II) addition

4 g of wet sand from one of the columns with 50 mL of tap water, 150 µL of Trace Elements solution, and 500 µL of 100 nM K-phosphate buffer solution (pH of 7.5) were placed in a horizontal flask shaker (Edmund Bühler GmbH, Germany) at 100 rpm. 1 mL of feeding solution (100 mg/L NH_4-N + 87 mg/L K_2HPO_4) was added at time zero, and ammonia consumption was monitored for 4 hours.

300 µL of 1 g/L of Fe^{2+} (pH of 2) were dosed every 30 min to understand the effect of iron on the ammonia consumption rate.

The control condition consisted of adding Milli-Q water acidified at a pH of 2 to replace the iron solution that pH and dilution would not interfere with the results.

Duplicates were made for each of the conditions.

Samples were taken at times 0.5h (not to misinterpret any ammonia adsorption onto the sand grains as consumption), 1h, 2h, 3h, and 4h.

3.3.2 Evaluation of ROS quenchers addition

ROS quenchers such as tempol (4-hydroxy-TEMPO), mannitol, and catalase were added to the batch flasks to study if iron inhibition was due to the formation of Reactive Oxygen Species. The protocol was adapted from Brinkman et al. (2016).

4 g of wet sand with 50 mL of tap water, 150 µL of Trace Elements solution, and 500 µL of 100 nM K-phosphate buffer solution (pH of 7.5) were placed in a horizontal flask shaker (Edmund Bühler GmbH, Germany) at 100 rpm. 1 mL of feeding solution (100 mg/L NH_4-N + 87 mg/L K_2HPO_4) was added at time zero, and ammonia consumption was monitored for 4 hours.

Four conditions were tested:

1. Addition of 75 µL of 4 g/L of Fe^{2+} (pH of 2) every 30 min;
2. Addition of 75 µL of the same iron solution + 254 µL of 4 g/L of tempol solution every 30 min;
3. Addition of 75 µL of the same iron solution + 254 µL of 215 g/L of mannitol solution every 30 min;
4. Addition of 75 µL of the same iron solution + 254 µL of 0.4 g/L of catalase (30 000 U/mg) solution every 30 min.

The control conditions included adding 75 µL of Milli-Q water acidified at a pH of 2 to replace the iron solution and adding 254 µL of neutral Milli-Q to substitute the Quencher's solutions.

Duplicates were made for each of the conditions.

Samples were taken at times 0.5h (not to misinterpret any ammonia adsorption onto the sand grains as consumption), 1h, 2h, 3h, and 4h.

3.4 Analytical Procedures

Chemical analyses on ammonium, nitrite, and nitrate content were performed in the Gallery Discrete Analyzer equipment (ThermoFisher, USA).

Sand grains were visualized under the Digital Microscope VHX-5000 with a VH-Z20UR lens (Keyence, Japan).

The data were plotted and statistically analyzed with GraphPad Prism software (Dotmatics, UK), which uses a statistical method equivalent to ANCOVA (Analysis of Covariance) to determine if the slopes between two linear regressions are significantly different (GraphPad Prism, 2022). A significant difference was considered when the p-value was inferior to 0.05.

Chapter 4

Results and Discussion

4.1 Columns ripened exclusively in the presence of FeOx-coated sand

Columns' inoculation took 25 days. However, each column responded and developed differently.

Circulation of the first inoculation solution, composed of ammonia-oxidizing microorganisms present in a DWTP's sand grains, resulted in successfully activating two out of three columns.

The second and third inoculation procedures (with activated sludge) had practically no effect on the ammonia consumption profile.

Figure 4.1 summarizes the timeline throughout the 25 days of the start-up period, including the moments of each inoculation and when ammonia consumption appeared for the first time in each column.

The columns are composed of only FeOx-coated sand, a mixture of FeOx-coated sand with virgin quartz sand, and only virgin quartz sand, respectively, as described in 3.1.

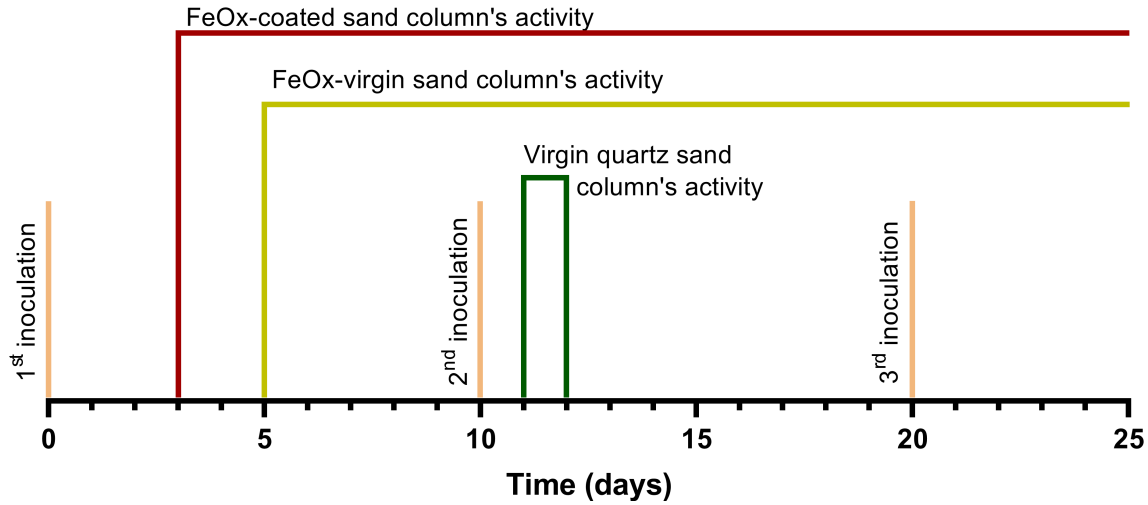

Figure 4.1: Timeline of the 25 days of the inoculation procedure. Light orange lines represent the time of each inoculation, whereas the red, yellow, and green bars represent the period of ammonia consumption of FeOx-coated sand, FeOx-virgin sand, and Virgin quartz sand columns, respectively.

FeOx-coated sand column was the first column to report activity, i.e., ammonia

consumption, followed by FeOx-virgin sand column. Virgin quartz sand column showed no signs of consumption, except for days 11 and 12 when ammonia was consumed, and nitrite was formed and subsequently transformed into nitrate.

An accumulation of activated sludge accompanied this limited period of activity on the top of virgin quartz sand's supernatant and bed, as exemplified by Figure 4.2. This layer remained after the surge of activity and after several attempts to force it through the bed, indicating that the microorganisms could or would not adhere to the virgin sand grains.

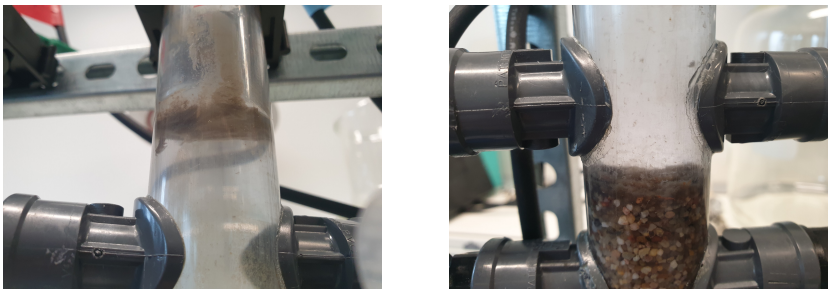

(a) Activated sludge on top of column's supernatant.

(b) Activated sludge on top of column's bed.

Figure 4.2: Layer of activated sludge formed on virgin quartz sand column after the second inoculation.

Moreover, since FeOx-coated sand and FeOx-virgin sand columns were the only ones containing iron oxides as a filter media, results suggest no FeOx-induced inhibition and a possible enhancement of the start-up period of rapid sand filtration upon their presence.

These results confirmed the observations of Gülay et al. (2014), who revealed that higher amounts of mineral coating could increase the biologically available surface area and the ammonia removal rate in RSF systems.

Although colonization of virgin sand is naturally possible and has already been reproduced (Breda, 2019; Bruins et al., 2015), no studies have tried to perform it without the presence or formation of mineral oxides.

4.2 FeOx-coating as a possible key to microbial development in RSF

For 30 days, the ammonia removal profile of the three columns was studied.

The FeOx-coated sand column was the first to achieve complete ammonia removal (after only 11 days of continuous flow), followed by the FeOx-virgin sand column (only on the 29^{th} day), as illustrated in Figure 4.3a. By comparing the removal profiles of both columns, it is clear to perceive that the FeOx-coated sand column developed faster than the FeOx-virgin sand column, indicating that FeOx-coating onto the sand grains does not harm AOM nor hinder the ammonia oxidation process.

Besides the difference in the start-up time between the two columns, they have also undergone ripening. Figure 4.3b compares the bed height at which 40% ammonia removal occurred between the FeOx-coated sand and the FeOx-virgin sand column. In the beginning, the water had to go through almost the entire column to achieve the desired removal capacity. However, as time goes by, the columns mature, and the microorganisms grow within the bed, increasing ammonia consumption and

decreasing the amount of bed necessary to achieve it. Again, it is clear to distinguish the evolution and maturation from the two columns, supporting the hypothesis that FeOx-coated sand does not hinder ammonia oxidation and hastens its ripening time.

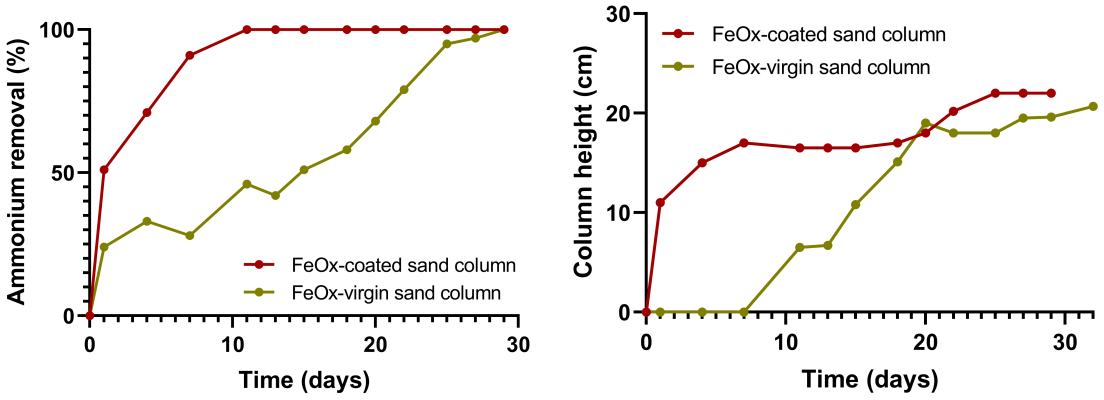

(a) (b)

Figure 4.3: (a) Full ammonia removal evolution of FeOx-coated sand (red) and FeOx-virgin sand (yellow) columns throughout experiment time, and (b) Bed height of FeOx-coated sand (red) and FeOx-virgin sand (yellow) columns at which 40% ammonia removal is achieved throughout time

Contrarily to the previously mentioned columns, no ammonia was consumed in the virgin quartz sand column after 20 days of continuous operation. After 46 days (accounting for inoculation time) of no activity, the influent was switched from tap water + growth medium to the effluent of FeOx-coated sand column + growth medium.

(a) Virgin quartz sand grains' sample from FeOx-virgin sand column.

(b) Virgin quartz sand grains' sample from virgin-quartz sand column.

Figure 4.4: Difference of microscopical pictures from FeOx-virgin sand column containing adsorbed iron oxides (a) and from virgin quartz sand column containing no oxides adsorption (b).

This change was intended to mimic the colonization process that unintentionally occurred in the FeOx-virgin sand column. As observed in Figure B.1b of Appendix B, there is consumption in the bottom half of this column. To understand why there was consumption in this section composed of only virgin quartz sand, but no consumption on the virgin quartz sand column, both virgin sands were compared

under the microscope (Figure 4.4). Results showed a higher amount of iron oxides in the virgin quartz sand from the bottom half of the FeOx-virgin sand column (Figure 4.4a), and no iron oxides in the virgin quartz sand column (Figure 4.4b), leading to the belief that the presence of oxides may be essential for the attachment and proliferation of microorganisms. Thus, to further inoculate the column with no activity, the influent was switched.

After 8 days of this change, 100% ammonia removal was achieved, as shown in Figure 4.5. From that moment on, the influent was again replaced by tap water + growth medium, which abruptly decreased the removal capacity.

The removal capacity stabilized at around 10%, without any evidence of increasing with time. It is hypothesized that the sharp increase in ammonia consumption was caused by planktonic cells present in the effluent of the FeOx-coated sand column. Therefore, once tap water was used as an influent, the planktonic cells were slowly released, explaining the decrease in ammonia removal. However, ammonia removal stabilized at $(12 \pm 2)\%$ during the following 18 days of operation, proving not only that AOM colonized the sand grains but also that this colonization was only possible after the presence of FeOx in the column.

Considering that after the first three inoculation attempts, there was no stable ammonia consumption in the virgin quartz sand column and that this stable consumption was only achieved with this latter procedure, FeOx-coating may play a central role in the microbial development of RSF systems.

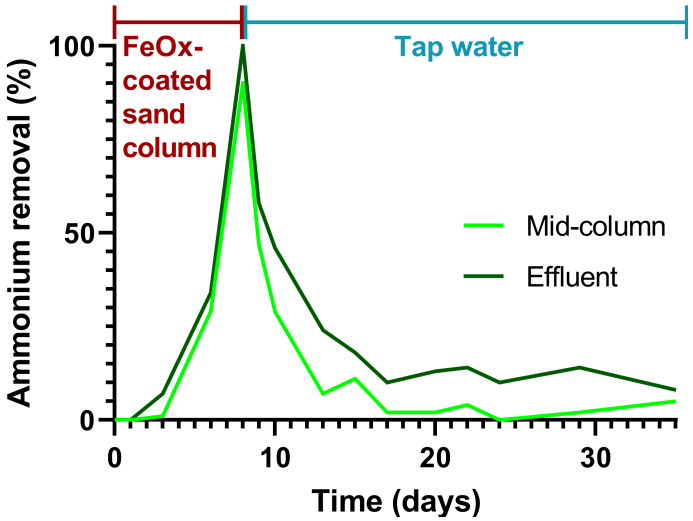

Figure 4.5: Evolution of the ammonia removal capacity of virgin quartz sand column's mid-height and effluent after the influent swap.

Although providing a good surface for microbial growth due to their high adsorption capacity, high porosity, and opposite zeta potentials with bacteria (as already mentioned in Subsection 2.4.1), these findings alone are not enough to prove the formulated hypothesis.

Thus, new studies to prove the necessity of these surfaces as a way of potentiating microbial attachment are required. Chapter 6 provides some recommendations for this purpose.

4.3 Reactive Oxygen Species are not responsible for ammonia oxidation inhibition

4.3.1 Iron(II) additions inhibit the maximum ammonia removal rate

Figure 4.6 presents the ammonia consumption throughout the four hours of the experiment.

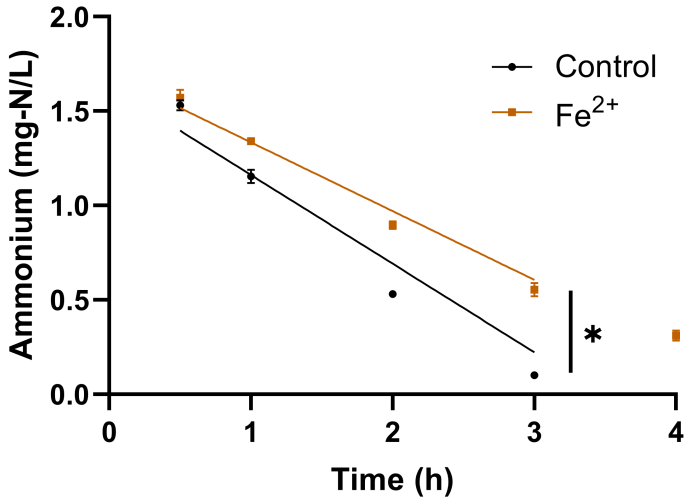

Figure 4.6: Consumption of ammonium throughout the experimental time between conditions control (black) and addition of iron(II) every 30 minutes (brown). * represents a statistically significant difference of $p<0.05$.

The consumption rates were only calculated between 0.5 h and 3 h so that only zero-order reaction kinetics were considered. These values can be found in Table B.1.

Results indicate a significant difference ($p=0.017$) between the addition of Fe^{2+} every 30 minutes and the control condition, proving that iron(II) inhibited ammonia oxidation.

This finding demonstrates that the ammonia removal hindrance found in full-scale RSF is highly likely due to the presence of iron(II) in the top part of the filter, as speculated.

However, what triggers this inhibition remains to be discovered.

4.3.2 ROS quenchers do not prevent inhibition

Tempol, mannitol, and catalase are some very well-known ROS quenchers (André et al., 2017; Brinkman et al., 2016; Kim et al., 2016; Santos et al., 2012; Wilcox, 2010; Wood et al., 2001).

Figure 4.7 compares control with or without ROS quenchers and their respective conditions with iron, thus eliminating the compounds' interference with the ammonia oxidation process. Once again, consumption rates were only calculated between 0.5 h and 3 h, as explained in the previous subsection. The linear regressions and comparison of all conditions can be consulted in Appendix B.4.

When analyzing the figure, tempol and mannitol appear to exert an effect when added to the control condition ($p=0.002$ and $p=0.03$, respectively). Catalase, on the other hand, does not have any interference with the control condition ($p=0.5$).

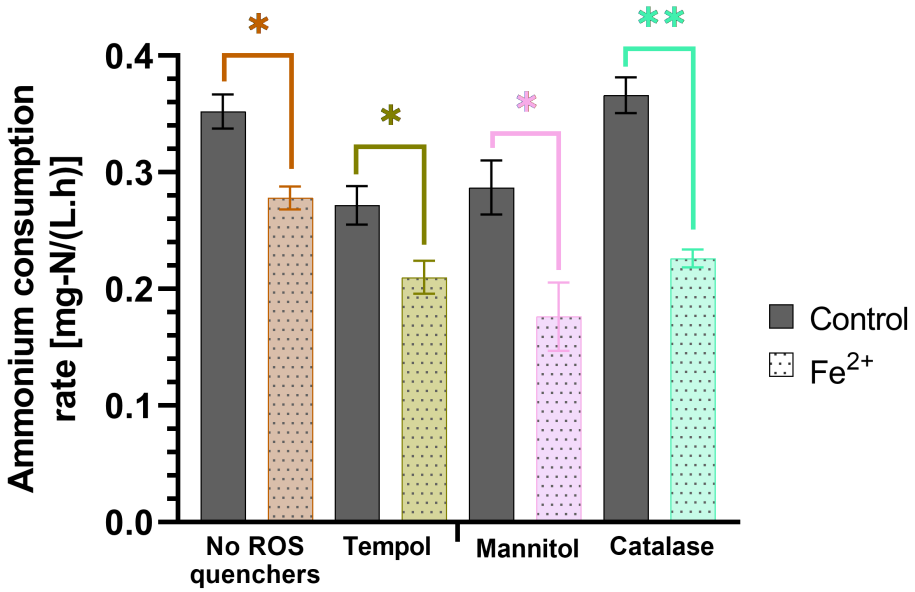

Figure 4.7: Ammonium consumption rates of all conditions tested. * represents a statistically significant difference of $p<0.05$, and ** a statistically significant difference of $p<0.0001$.

Catalase is an enzyme that catalyzes the reaction of hydrogen peroxide into $H_2O_2 + \frac{1}{2} O_2$ (Kim et al., 2016; Santos et al., 2012; Wood et al., 2001). As it is natural to the nitrifying community, it was expected not to harm AOM nor the ammonia oxidation process.

Tempol and mannitol, however, may be toxic to microbial cells in certain conditions.

J. Cai et al. (2018) studied the effect of different Tempol concentrations on gut microbiota *in vitro*. They discovered that metabolic activity and membrane integrity would be compromised with concentrations over 0.01 mg/mL and that membrane depolarisation would occur at concentrations above 1 mg/mL. Considering that with every 30-minute Tempol addition, concentration increased by 0.17 mg/L and that by the end of the experiment, the final concentration was 1.4 mg/L, microbial toxicity could have occurred.

Additionally, Hommes et al. (2003) also tried to grow *Nitrosomonas europaea*, a nitrifying bacteria, in several organic carbon sources. Even though they succeeded in the presence of fructose or pyruvate as a sole carbon source, growth with mannitol (911 mg/L, 1.8 g/L, and 9.1 g/L) and other substances was not possible. The authors claimed that the bacteria could have attempted to replace NH_3 with these organic sources as an energy substrate instead of a carbon substrate (Hommes et al., 2003). Since tap water has enough carbonate as a carbon source for the nitrifiers to uptake (Evides, 2021a; 2021b), they should not attempt to substitute it with mannitol. Nevertheless, under the stress that iron exerts on them, this possibility should not be disregarded. Furthermore, it is essential to consider that the MIC (Minimum Inhibitory Concentration) of Mannitol in *E. coli* is 102.4 mg/mL (Inaba et al., 2020). Given that every 30-minute Mannitol addition resulted in an increase of 9.1 mg/mL in the solution and that, after 4 hours, the concentration was 72.9 mg/mL, there might be a possibility of inhibitory effects occurrence, potentiated by the pre-existing inhibition of iron.

These quenchers' interference with the ammonia oxidation process was not ac-

counted for when designing the experiments. Nonetheless, when comparing the tempol and mannitol's control condition to their iron condition, the difference is also significant (p=0.01 and p=0.009, respectively). This indicates that the presence of iron(II) is still harming ammonia oxidation, suggesting that the quenchers were unable to prevent the iron inhibition over the ammonia oxidation process.

Considering that the quenchers neutralize the radical species formed upon iron oxidation, these results indicate that ROS are not responsible for the observed inhibition.

Thus, as illustrated, iron significantly hinders ammonia oxidation even in the presence of ROS scavengers.

4.4 Adsorption of newly formed iron oxides can disturb the microbial community

To test if the ammonia removal profile would change in the presence of iron(II), after reaching 100% ammonia removal capacity, the FeOx-virgin sand column was subjected to a moderate concentration of Fe^{2+} (3 mg/L) for 1 day.

Figure 4.8 displays the ammonia removal capacity profile before the addition of iron (black), with the iron addition (red), and the recovery period of 3 weeks afterwards (shades of green).

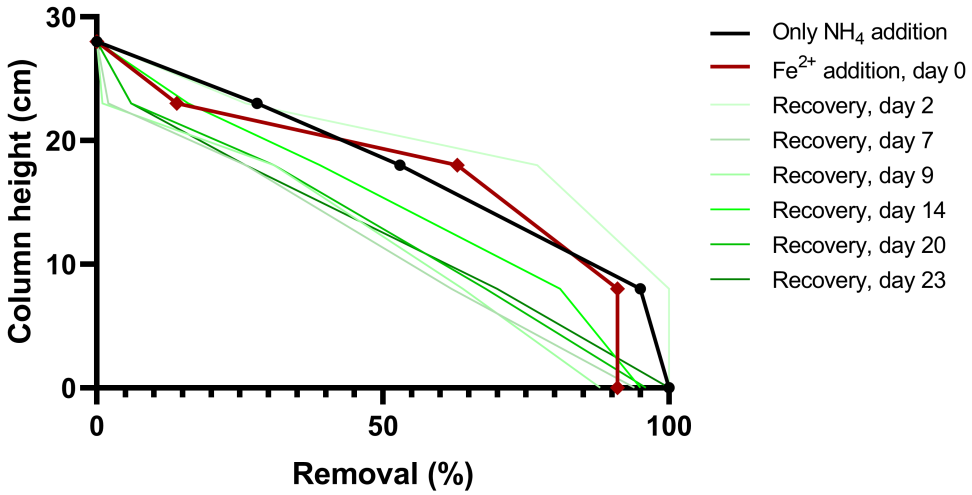

Figure 4.8: FeOx-virgin sand column's ammonia removal profile before (black), during (red), and after (shades of green) iron(II) addition.

Results suggest a hold of ammonia oxidation in the filter's top part when iron is added between the first and third point (height of 28 cm). When comparing the red and black lines, it becomes clear that between these two points, the black line's removal capacity is higher (reaching almost 30% removal), whereas the red line only achieves 15%. This indicates that in the region where iron is oxidized, ammonia removal capacity decreases.

Moreover, even after stopping Fe^{2+} inflow, the profile never fully recovered after the following 23 days.

Considering the brief lifetime of ROS and the full development of Column 2's removal profile in 4 weeks (see Figure B.1b), it can be presumed that if these species were the primary cause of ammonia oxidation inhibition, the column should be able of a faster recovery.

Thus, it can be hypothesized that the trigger for this phenomenon might be the newly formed iron oxides that form on top of the biofilm, hindering it. In fact, Schwegmann et al. (2010) studied the effect of adsorption of iron oxide nanoparticles onto E. coli and observed 70% toxicity at only 0.23 mg/L of FeOx and 99% toxicity at 7.2 mg/L of FeOx. Due to the opposite zeta potentials of bacteria and iron oxides (already mentioned in Subsection 2.4.1), there is a possibility of FeOx's adherence to the biofilm of the sand grains, limiting their activity and preventing their development, thus explaining the results.

Moreover, Tong et al. (2022) also found that at Fe^{2+} concentrations below 2.8 mg/L, bacterial manganese oxidation would be inhibited. They attributed this suppression to the attachment of iron-(hydro)oxides onto the bacterial surface, damaging the cell membrane (Tong et al., 2022). This harm enables dissolved iron influx into the cell, hindering multicopper oxidases responsible for manganese oxidation (Tong et al., 2022).

These iron-(hydro)oxides were identified as ferrihydrite (Tong et al., 2022), the dominant form of iron oxides in RSF, as mentioned in Subsection 2.2.1. Moreover, since AMO and HCO (heme-copper oxidase) are copper-dependent enzymes during nitrification (Klotz et al., 2008), a similar process may also be happening in this system.

Nevertheless, recovery of the system should still be possible after stopping iron oxidation. If indeed ammonia-oxidizing microbial biofilm at the iron oxidation region was injured, and no further harmful agents are inflowing into the system, then it should be just a matter of time until full recovery is achieved.

Chapter 5

Conclusions

Over the past five months, the Master's student investigated iron's effect on the ammonia oxidation process of Rapid Sand Filters. The project aimed to understand whether iron oxides-coated sand or reactive oxygen species were the reason for the observed ammonia oxidation inhibition phenomenon at several full-scale Drinking Water Treatment Plants in The Netherlands.

Overall, the work allowed the following conclusions to be drawn:

1. Iron oxidation is the leading cause of inhibition in the ammonia oxidation process;
2. Iron oxides-coated sand grains are not responsible for that inhibition; contrary, they favoured the microbial colonization on the grains;
3. The formation of reactive oxygen species through Fenton or Fenton-like reactions during iron oxidation is also not responsible for the observed circumstance;
4. The most likely cause for hindrance is the newly formed iron oxides that attach to the surface of the microorganisms, hindering it.

Even though irrefutable proof of what mechanisms behind iron oxidation causes the phenomenon in rapid sand filters has not been achieved, the hypotheses were tested, and a new theory was formulated.

Thus, future work should focus on testing the new hypothesis, ensuring that the underlying reason is discovered to optimize the rapid sand filtration process.

Chapter 6

Future Recommendations

Even though the findings discovered throughout these past five months were exciting and allowed the understanding of which direction to continue research, more proof is needed to support them.

Therefore, some recommendations for future work will be discussed in this Chapter.

First, to prove the claims in Section 4.2, two approaches are suggested:

1. Set up two lab-scale RSF columns, each with different sand media - virgin quartz sand and FeOx-chemically-coated sand (protocol for the latter available from Aal et al., 2009). Connect the influents of both columns to the effluent of Column 3 used throughout this work - this will enable faster colonization of the two columns. Measure ammonia-oxidizing activity in both columns and stop feeding once the removal capacity reaches 100%. Analyze activity afterwards in both columns to understand if the column with FeOx-chemically-coated retained more activity than the virgin quartz column.
2. Once the activity has plateaued, sample sand grains from each column and microscopically observe if microorganisms colonized within the FeOx-coated zone or elsewhere. There are a few methods possible to achieve this goal. The first is using a Confocal Laser Scanning Microscope (CLSM) and staining the sand grains with a Live/Dead BacLight viability kit or a SYBR green I stain (see Figure 6.1) (Gülay et al., 2014; Probandt et al., 2018). The other is by using an Environmental Scanning Electron Microscope (E-SEM) (see Figure 6.2) (Gülay et al., 2014). Once irrefutable proof that the microorganisms colonize the mineral coating instead of the quartz surface, a considerable degree of certainty may be said about how FeOx are essential for microbial growth in RSF.

Second, to ensure that the batch tests comprising ROS quenchers were efficacious, a positive control should be performed.

Thus, running a set of batch tests in the same conditions as described in Subsection 3.3.2 with hydrogen peroxide instead of Fe^{2+} as a source of ROS is suggested.

As mentioned in Subsection 2.2.2, H_2O_2 is a well-known ROS capable of hindering ammonia oxidation. Hence, it is recommended to subject the sand grains to an inhibiting concentration of H_2O_2 and compare the obtained inhibition with conditions containing tempol, mannitol, and catalase.

If the ROS quenchers can neutralize the inhibitory effect of hydrogen peroxide in the ammonia oxidation, then more certainty is gained to support the previous results.

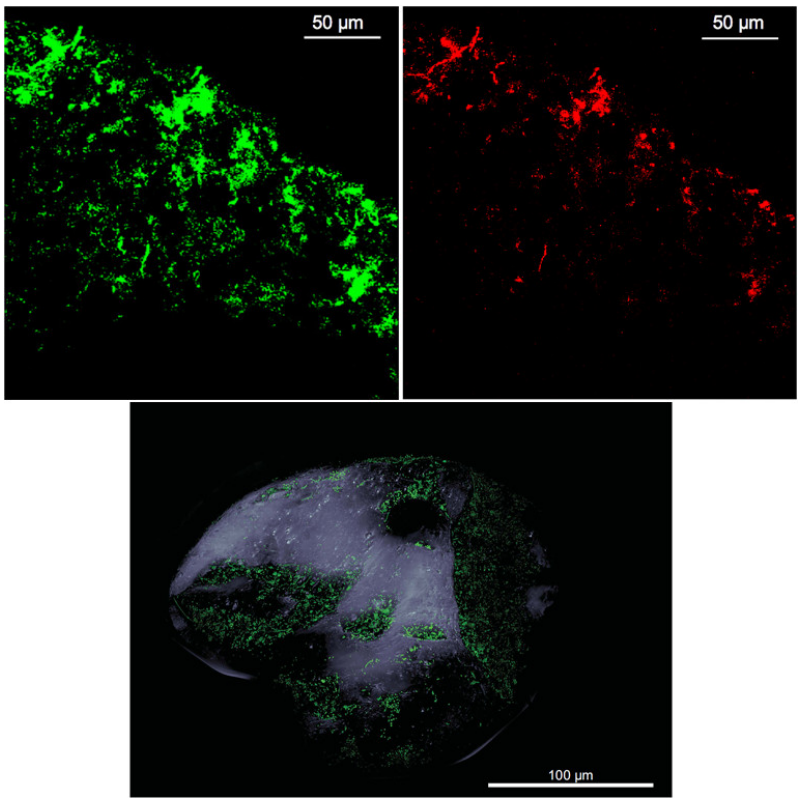

Figure 6.1: Confocal Laser Scanning Micrograph showing microbial colonization of a sand grain stained with Live/Dead BacLight viability kit (top pictures, outer periphery of the grain; retrieved from Gülay et al., 2014) and with a SYBR green I stain (bottom picture; retrieved from Probandt et al., 2018).

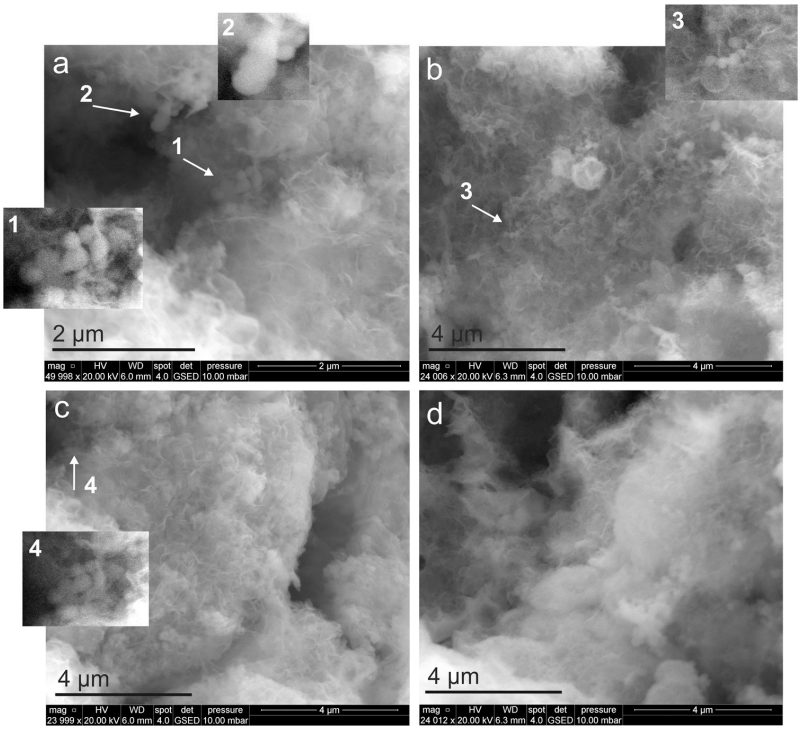

Figure 6.2: Environmental Scanning Electron Micrograph showing microbial colonization of internal pores of a sand grain. Coccoid cell-like structures are indicated by arrows and numbers. Retrieved from Gülay et al., 2014.

Third, to understand if, in fact, the newly formed FeOx sediment on top of bacterial biofilm is hindering the cell membrane, an approach similar to the one described in the first part of this Chapter is recommended.

To do so, a lab-scale RSF column should be assembled with identical conditions described in Subsection 3.2.2. FeOx-coated sand should be used as filter media, and iron(III) should be used as influent (to mimic the formation of iron-(hydro)oxides) and dosed for a longer period. Afterwards, sand grains samples should be taken from the top (where iron oxidation will occur) and bottom parts of the filter, stained with a Live/Dead BacLight viability kit, and visualized under a CLSM.

If the results indicate that biofilm from the top has significantly higher dead cells than that on the bottom, a step further has been taken to prove the hypothesis.

Alternatively, batch experiments could be run similarly to Section 3.3, replacing the iron(II) solution for iron(III). Likewise, if the same rate of inhibition is observed by dosing iron-(hydro)oxides, more confidence will be that this is indeed the cause of hindrance observed in RSF systems.

References

Aal, G. A., Atekwana, E., Radzikowski, S., & Rossbach, S. (2009). Effect of bacterial adsorption on low frequency electrical properties of clean quartz sands and iron-oxide coated sands. *Geophysical Research Letters*, *36*(4), 1–5. https://doi.org/10.1029/2008GL036196

Águas de Portugal. (2015). O ciclo urbano da água. Retrieved February 16, 2022, from https://www.adp.pt/pt/atividade/o-que-fazemos/o-ciclo-urbano-da-agua/?id=28

Ameta, R., Chohadia, A. K., Jain, A., & Punjabi, P. B. (2018). *Fenton and Photo-Fenton Processes*. https://doi.org/10.1016/B978-0-12-810499-6.00003-6

André, P., & Villain, F. (2017). Free radical scavenging properties of mannitol and its role as a constituent of hyaluronic acid fillers: a literature review. *International Journal of Cosmetic Science*, *39*(4), 355–360. https://doi.org/10.1111/ics.12386

Bender, D. A. (2012). Nitrogen Metabolism. *Amino acid metabolism* (pp. 1–65). https://doi.org/10.1002/9781118357514.ch1

Bitton, G. (2014). *Drinking Water Production and Distribution*. John Wiley Sons, Inc.

Breda, I. L. R. (2019). *Manganese removal in drinking water biofilters: from start-up to matured filters* (Doctoral dissertation). Aalborg Universitet.

Brinkman, C. L., Schmidt-Malan, S. M., Karau, M. J., Greenwood-Quaintance, K., Hassett, D. J., Mandrekar, J. N., & Patel, R. (2016). Exposure of bacterial biofilms to electrical current leads to cell death mediated in part by reactive oxygen species. *PLoS ONE*, *11*(12), 1–23. https://doi.org/10.1371/journal.pone.0168595

Brown, J., Wre, D., Sharp, R. R., & Ph, D. (2013). Nitrification. *Operation of nutrient removal facilities - wef manual of practice no. 37*.

Bruins, J. H., Petrusevski, B., Slokar, Y. M., Huysman, K., Joris, K., Kruithof, J. C., & Kennedy, M. D. (2015). Reduction of ripening time of full-scale manganese removal filters with manganese oxide-coated media. *Journal of Water Supply: Research and Technology - AQUA*, *64*(4), 434–441. https://doi.org/10.2166/aqua.2015.117

Cai, J., Nichols, R. G., Koo, I., Kalikow, Z. A., Zhang, L., Tian, Y., Zhang, J., Smith, P. B., & Patterson, A. D. (2018). Multiplatform Physiologic and Metabolic Phenotyping Reveals Microbial Toxicity. *mSystems*, *3*(6). https://doi.org/10.1128/msystems.00123-18

Cai, Y., Li, D., Liang, Y., Luo, Y., Zeng, H., & Zhang, J. (2015). Effective start-up biofiltration method for Fe, Mn, and ammonia removal and bacterial community analysis. *Bioresource Technology*, *176*, 149–155. https://doi.org/10.1016/j.biortech.2014.11.025

Caranto, J. D., & Lancaster, K. M. (2017). Nitric oxide is an obligate bacterial nitrification intermediate produced by hydroxylamine oxidoreductase. *Proceedings of the National Academy of Sciences of the United States of America*, *114*(31), 8217–8222. https://doi.org/10.1073/pnas.1704504114

Cornell, R. M., & Schwertmann, U. (2003). *Introduction to the Iron Oxides*. https://doi.org/10.1002/3527602097.ch1

Daims, H., Lebedeva, E. V., Pjevac, P., Han, P., Herbold, C., Albertsen, M., Jehmlich, N., Palatinszky, M., Vierheilig, J., Bulaev, A., Kirkegaard, R. H., Von Bergen, M., Rattei, T., Bendinger, B., Nielsen, P. H., & Wagner, M. (2015). Complete nitrification by Nitrospira bacteria. *Nature*, *528*(7583), 504–509. https://doi.org/10.1038/nature16461

de Moel, P. J., Verberk, J. Q. J. C., & van Dijk, J. C. (2006). *Drinking Water: Principles and Practices.pdf* (Tjan Kwang Wei, Ed.). World Scientific Publishing Co. Pte. Ltd.

de Vet, W. W., Dinkla, I. J., Muyzer, G., Rietveld, L. C., & van Loosdrecht, M. C. (2009). Molecular characterization of microbial populations in groundwater sources and sand filters for drinking water production. *Water Research*, *43*(1), 182–194. https://doi.org/10.1016/j.watres.2008.09.038

de Vet, W. W., Kleerebezem, R., van der Wielen, P. W., Rietveld, L. C., & van Loosdrecht, M. C. (2011). Assessment of nitrification in groundwater filters for drinking water production by qPCR and activity measurement. *Water Research*, *45*(13), 4008–4018. https://doi.org/10.1016/j.watres.2011.05.005

de Vet, W. W., Rietveld, L. C., & van Loosdrecht, M. C. (2009). Influence of iron on nitrification in full-scale drinking water trickling filters. *Journal of Water Supply: Research and Technology - AQUA*, *58*(4), 247–256. https://doi.org/10.2166/aqua.2009.115

de Vet, W. W., van Genuchten, C. C., van Loosdrecht, M. C., & van Dijk, J. C. (2010). Water quality and treatment of river bank filtrate. *Drinking Water Engineering and Science*, *3*(1), 79–90. https://doi.org/10.5194/dwes-3-79-2010

Emmenegger, L., Whitney King, D., Sigg, L., & Sulzberger, B. (1998). Oxidation kinetics of Fe(II) in a eutrophic swiss lake. *Environmental Science and Technology*, *32*(19), 2990–2996. https://doi.org/10.1021/es980207g

Etcheberry, T., Lavigne, M. P., Trias, R., Brunner, S., Zuluaga, J. T., Di Gioia, L., & Paul, E. (2022). Start-up strategies for nitrification and manganese oxidation on a single stage RSF for drinking water production. *Water Supply*, *22*(2), 2243–2256. https://doi.org/10.2166/ws.2021.369

Evides. (2021a). *Productielocatie Berenplaat - Gemiddelde drinkwaterkwaliteit per maand en voortschrijdend jaar* (tech. rep.). https://www.evides.nl/drinkwater/waterkwaliteit-en-hardheid/stoffen-in-drinkwater

Evides. (2021b). *Productielocatie Kralingen - Gemiddelde drinkwaterkwaliteit per maand en voortschrijdend jaar* (tech. rep.). https://www.evides.nl/drinkwater/waterkwaliteit-en-hardheid/stoffen-in-drinkwater

Gerardi, M. H. (2016a). Nitrification and Limiting Factors. *Operator's guide to biological nutrient removal (bnr) in the activated sludge process* (pp. 58–80).

Gerardi, M. H. (2016b). Nitrifying Bacteria. *Operator's guide to biological nutrient removal (bnr) in the activated sludge process* (pp. 51–57).

GraphPad Prism. (2022). GraphPad Prism 9 Curve Fitting Guide - Comparing slopes and intercepts. Retrieved June 24, 2022, from https://www.graphpad.com/guides/prism/latest/curve-fitting/reg_comparingslopesandintercepts.htm

Gülay, A., Musovic, S., Albrechtsen, H. J., Al-Soud, W. A., Sørensen, S. J., & Smets, B. F. (2016). Ecological patterns, diversity and core taxa of microbial communities in groundwater-fed rapid gravity filters. *ISME Journal*, *10*(9), 2209–2222. https://doi.org/10.1038/ismej.2016.16

Gülay, A., Tatari, K., Musovic, S., Mateiu, R. V., Albrechtsen, H. J., & Smets, B. F. (2014). Internal porosity of mineral coating supports microbial activity in rapid sand filters for groundwater treatment. *Applied and Environmental Microbiology*, *80*(22), 7010–7020. https://doi.org/10.1128/AEM.01959-14

Hammes, F., Velten, S., Egli, T., & Juhna, T. (2011). *Biotreatment of Drinking Water* (Second Edi, Vol. 6). Elsevier B.V. https://doi.org/10.1016/B978-0-08-088504-9.00386-X

He, J., Yang, X., Men, B., & Wang, D. (2016). Interfacial mechanisms of heterogeneous Fenton reactions catalyzed by iron-based materials: A review. *Journal of Environmental Sciences (China)*, *39*, 97–109. https://doi.org/10.1016/j.jes.2015.12.003

Hommes, N. G., Sayavedra-Soto, L. A., & Arp, D. J. (2003). Chemolithoorganotrophic Growth of Nitrosomonas europaea on Fructose. *Journal of Bacteriology*, *185*(23), 6809–6814. https://doi.org/10.1128/JB.185.23.6809-6814.2003

Inaba, K., Minami, M., Yamaguchi, M., Goto, R., Otake, H., Kotake, T., & Nagai, N. (2020). Effects of the ophthalmic additive mannitol on antimicrobial activity and corneal toxicity of various preservatives. *Chemical and Pharmaceutical Bulletin*, *68*(11), 1069–1073. https://doi.org/10.1248/cpb.c20-00540

Kim, J.-g., Park, S.-j., Sinninghe, J. S., Schouten, S., Rijpstra, W. I. C., & Jung, M.-y. (2016). Hydrogen peroxide detoxification is a key mechanism for growth of ammonia-oxidizing archaea. *113*(28), 7888–7893. https://doi.org/10.1073/pnas.1605501113

King, D. W., Lounsbury, H. A., & Millero, F. J. (1995). Rates and Mechanism of Fe(II) Oxidation at Nanomolar Total Iron Concentrations. *Environmental Science and Technology*, *29*(3), 818–824. https://doi.org/10.1021/es00003a033

Klotz, M. G., & Stein, L. Y. (2008). Nitrifier genomics and evolution of the nitrogen cycle. *FEMS Microbiology Letters*, *278*(2), 146–156. https://doi.org/10.1111/j.1574-6968.2007.00970.x

Kuypers, M. M., Marchant, H. K., & Kartal, B. (2018). The microbial nitrogen-cycling network. *Nature Reviews Microbiology*, *16*(5), 263–276. https://doi.org/10.1038/nrmicro.2018.9

Madigan, M. T., Bender, K. S., Buckley, D. H., Sattley, W. M., & Stahl, D. A. (2019). *Brock biology of microorganisms* (P. E. Limited, Ed.; Fifhteenth). Pearson.

Michel, M. M., Reczek, L., Papciak, D., Wlodarczyk-Makula, M., Siwiec, T., & Trach, Y. (2020). Mineral materials coated with and consisting of MnOx - Characteristics and application of filter media for groundwater treatment: A Review. *Materials*, *13*(10), 1–35. https://doi.org/10.3390/ma13102232

Mills, A. L., Herman, J. S., Hornberger, G. M., & DeJesus, T. H. (1994). Effect of solution ionic strength and iron coatings on mineral grains on the sorption of bacterial cells to quartz sand. *Applied and Environmental Microbiology*, *60*(9), 3300–3306. https://doi.org/10.1128/aem.60.9.3300-3306.1994

Morris, J. J., Rose, A. L., & Lu, Z. (2022). Reactive oxygen species in the world ocean and their impacts on marine ecosystems. *Redox Biology*, *52*(October 2021), 102285. https://doi.org/10.1016/j.redox.2022.102285

Ons Water. (n.d.). How is drinking water made? † Our water. Retrieved February 18, 2022, from https://www.onswater.nl/onderwerpen/hoe-wordt-drinkwater-gemaakt

Pereira, M. C., Oliveira, L. C. A., & Murad, E. (2012). Iron oxide catalysts: Fenton and Fentonlike reactions – a review. *Clay Minerals*, *47*(3), 285–302. https://doi.org/10.1180/claymin.2012.047.3.01

Pham, A. L. T. (2012). *Activation of Hydrogen Peroxide by Iron-Containing Minerals and Catalysts in Circumneutral pH Solutions : Implications for ex situ and in situ Treatment of Contaminated Water and Soil* (PhD Thesis). University of California, Berkeley.

Probandt, D., Eickhorst, T., Ellrott, A., Amann, R., & Knittel, K. (2018). Microbial life on a sand grain: From bulk sediment to single grains. *ISME Journal*, *12*(2), 623–633. https://doi.org/10.1038/ismej.2017.197

Qin, S., Ma, F., Huang, P., & Yang, J. (2009). Fe (II) and Mn (II) removal from drilled well water: A case study from a biological treatment unit in Harbin. *Desalination*, *245*(1-3), 183–193. https://doi.org/10.1016/j.desal.2008.04.048

Ramsay, L., Du, F., Lund, M., He, H., & Søborg, D. A. (2021). Grain displacement during backwash of drinking water filters. *Water Science and Technology: Water Supply*, *21*(1), 356–367. https://doi.org/10.2166/ws.2020.300

Robertson, G. P., & Groffman, P. M. (2015). Nitrogen Transformations. *Soil microbiology ecology and biochemistry* (4th ed., pp. 421–446). Elsevier Inc. https://doi.org/10.1016/B978-0-12-415955-6.00014-1

Rose, A. L., & Waite, T. D. (2002). Kinetic model for FE(II) oxidation in seawater in the absence and presence of natural organic matter. *Environmental Science and Technology*, *36*(3), 433–444. https://doi.org/10.1021/es0109242

Santos, A. L., Gomes, N. C., Henriques, I., Almeida, A., Correia, A., & Cunha, Â. (2012). Contribution of reactive oxygen species to UV-B-induced damage in bacteria. *Journal of Photochemistry and Photobiology B: Biology*, *117*, 40–46. https://doi.org/10.1016/j.jphotobiol.2012.08.016

Sayavedra-Soto, L. A., Vajrala, N., & Arp, D. J. (2011). Dissecting Iron Uptake and Homeostasis in Nitrosomonas europaea. *Methods in enzymology: Research on nitrification and related processes, part a* (1st ed., pp. 403–428). Elsevier Inc. https://doi.org/10.1016/B978-0-12-381294-0.00018-3

Schwegmann, H., Feitz, A. J., & Frimmel, F. H. (2010). Influence of the zeta potential on the sorption and toxicity of iron oxide nanoparticles on S. cerevisiae and E. coli. *Journal of Colloid and Interface Science*, *347*(1), 43–48. https://doi.org/10.1016/j.jcis.2010.02.028

Schwertmann, U., & Fechter, H. (1982). The point of zero charge of natural and synthetic ferrihydrites and its relation to adsorbed silicate. *Clay Minerals*, *17*(4), 471–476. https://doi.org/10.1180/claymin.1982.017.4.10

Sharma, S. K., Greetham, M. R., & Schippers, J. C. (1999). Adsorption of iron(II) onto filter media. *Journal of Water Supply: Research and Technology - AQUA*, *48*(3), 84–91. https://doi.org/10.1046/j.1365-2087.1999.00131.x

Sharma, S. K., Petrusevski, B., & Schippers, J. C. (2002). Characterisation of coated sand from iron removal plants. *Water Science and Technology: Water Supply*, *2*(2), 247–257. https://doi.org/10.2166/ws.2002.0070

Smeets, P. W. M. H., Medema, G. J., & van Dijk, J. C. (2009). The Dutch secret: how to provide safe drinking water without chlorine in the Netherlands. *Drinking Water Engineering and Science*, *2*(1), 1–14. https://doi.org/10.5194/dwes-2-1-2009

Soler-Jofra, A., Picioreanu, C., Yu, R., Chandran, K., van Loosdrecht, M. C., & Pérez, J. (2018). Importance of hydroxylamine in abiotic N2O production during transient anoxia in planktonic axenic Nitrosomonas cultures. *Chemical Engineering Journal*, *335*(October 2017), 756–762. https://doi.org/10.1016/j.cej.2017.10.141

Stein, L. Y. (2019). Insights into the physiology of ammonia-oxidizing microorganisms. *Current Opinion in Chemical Biology*, *49*, 9–15. https://doi.org/10.1016/j.cbpa.2018.09.003

Stein, L. Y., & Klotz, M. G. (2016). The nitrogen cycle. *Current Biology*, *26*(3), R94–R98. https://doi.org/10.1016/j.cub.2015.12.021

Štembal, T., Markić, M., Briški, F., & Sipos, L. (2004). Rapid start-up of biofilters for removal of ammonium, iron and manganese from ground water. *Journal of Water Supply: Research and Technology - AQUA*, *53*(7), 509–518. https://doi.org/10.2166/aqua.2004.0040

Tatari, K., Smets, B. F., & Albrechtsen, H. (2013). A novel bench-scale column assay to investigate site-specific nitrification biokinetics in biological rapid sand filters. *Water Research*, *47*(16), 6380–6387. https://doi.org/10.1016/j.watres.2013.08.005

Tekerlekopoulou, A. G., Pavlou, S., & Vayenas, D. V. (2013). Removal of ammonium, iron and manganese from potable water in biofiltration units: A review. *Journal of Chemical Technology and Biotechnology*, *88*(5), 751–773. https://doi.org/10.1002/jctb.4031

Tolar, B. B., Powers, L. C., Miller, W. L., Wallsgrove, N. J., Popp, B. N., & Hollibaugh, J. T. (2016). Ammonia oxidation in the ocean can be inhibited by nanomolar concentrations of hydrogen peroxide. *Frontiers in Marine Science*, *3*(NOV), 1–16. https://doi.org/10.3389/fmars.2016.00237

Tong, M., Zhao, Y., Sun, Q., Li, P., Liu, H., & Yuan, S. (2022). Fe(II) oxygenation inhibits bacterial Mn(II) oxidation by P. putida MnB1 in groundwater under O2-perturbed conditions. *Journal of Hazardous Materials*, *435*(68), 128972. https://doi.org/10.1016/j.jhazmat.2022.128972

Truesdail, S. E., Lukasik, J., Farrah, S. R., Shah, D. O., & Dickinson, R. B. (1998). Analysis of bacterial deposition on metal (hydr)oxide-coated sand filter media. *Journal of Colloid and Interface Science*, *203*(2), 369–378. https://doi.org/10.1006/jcis.1998.5541

UN. (n.d.). Goal 6 — Department of Economic and Social Affairs. Retrieved February 17, 2022, from https://sdgs.un.org/goals/goal6

van Beek, C. G., Dusseldorp, J., Joris, K., Huysman, K., Leijssen, H., Schoonenberg Kegel, F., de Vet, W. W., van De Wetering, S., & Hofs, B. (2016). Contributions of homogeneous, heterogeneous and biological iron(II) oxidation in aeration and rapid sand filtration (RSF) in field sites. *Journal of Water Supply: Research and Technology - AQUA*, *65*(3), 195–207. https://doi.org/10.2166/aqua.2015.059

van Beek, C. G., Hiemstra, T., Hofs, B., Nederlof, M. M., van Paassen, J. A., & Reijnen, G. K. (2012). Homogeneous, heterogeneous and biological oxidation of iron(II) in rapid sand filtration. *Journal of Water Supply: Research and Technology - AQUA*, *61*(1), 1–13. https://doi.org/10.2166/aqua.2012.033

van Kessel, M. A., Speth, D. R., Albertsen, M., Nielsen, P. H., Op Den Camp, H. J., Kartal, B., Jetten, M. S., & Lücker, S. (2015). Complete nitrification by a single microorganism. *Nature*, *528*(7583), 555–559. https://doi.org/10.1038/nature16459

Vatansever, F., Avci, P., Vecchio, D., Gupta, A., Chandran, R., Karimi, M., Parizotto, A., Yin, R., Tegos, G. P., & Hamblin, M. R. (2013). Antimicrobial strategies centered around reactive oxygen species – bactericidal antibiotics, photodynamic therapy, and beyond. *FEMS Microbiology Reviews*, *37*(6), 955–989. https://doi.org/10.1111/1574-6976.12026

Vries, D., Korevaar, M., de Waal, L., & Ahmad, A. (2021). Impact of ionic composition of groundwater on oxidative iron precipitation. *Water Supply*, *00*(0), 1–9. https://doi.org/10.2166/ws.2021.406

Wakelin, S. A., Page, D. W., Pavelic, P., Gregg, A. L., & Dillon, P. J. (2010). Rich microbial communities inhabit water treatment biofilters and are differentially affected by filter type and sampling depth. *Water Science and Technology: Water Supply*, *10*(2), 145–156. https://doi.org/10.2166/ws.2010.570

Wang, J., de Ridder, D., van der Wal, A., & Sutton, N. B. (2021). Harnessing biodegradation potential of rapid sand filtration for organic micropollutant removal from drinking water: A review. *Critical Reviews in Environmental Science and Technology*, *51*(18), 2086–2118. https://doi.org/10.1080/10643389.2020.1771888

WHO. (2017). *Guidelines for Drinking-water Quality* (World Health Organization, Ed.; Fourth). WHO Library Cataloguing-in-Publication Data. https://www.who.int/publications/i/item/9789241549950

WHO. (2022). Drinking-water. Retrieved February 17, 2022, from https://www.who.int/news-room/fact-sheets/detail/drinking-water

Wilcox, C. S. (2010). Pharmacology Therapeutics Effects of tempol and redox-cycling nitroxides in models of oxidative stress. *Pharmacology and Therapeutics*, *126*(2), 119–145. https://doi.org/10.1016/j.pharmthera.2010.01.003

Wilson, C. L., Hinman, N. W., & Sheridan, R. P. (2000). Hydrogen Peroxide Formation and Decay in Iron-rich Geothermal Waters: The Relative Roles of Abiotic and Biotic Mechanisms. *Photochemistry and Photobiology*, *71*(6), 691. https://doi.org/10.1562/0031-8655(2000)071⟨0691:hpfadi⟩2.0.co;2

Wood, N. J., & Sörensen, J. (2001). Catalase and superoxide dismutase activity in ammonia-oxidising bacteria. *38*, 53–58.

Zannoni, D. (2004). *Advances in Photosynthesis and Respiration. Volume 16: Respiration in Archaea and Bacteria: Diversity of Prokaryotic Respiratory Systems.*

Zhang, Y., Love, N., Edwards, M., Zhang, Y. A. N., Love, N., & Edwards, M. (2009). Technology Nitrification in Drinking Water Systems. *Critical Reviews in Environmental Science and Technology*, *3389*. https://doi.org/10.1080/10643380701631739

Zhou, M., Oturan, M. A., & Sirés, I. (Eds.). (2018). *Electro-Fenton Processes: New Trends and Scale-Up* (1st ed.). Springer Nature Singapore. https://link.springer.com/book/10.1007/978-981-10-6406-7

Appendix A

Appendix

A.1 Columns Design and Filter Media

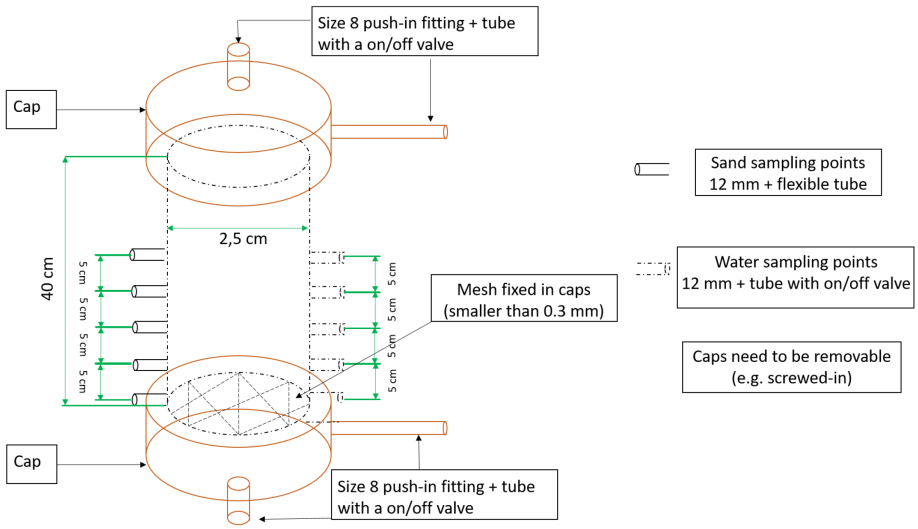

Figure A.1: Design of one column ordered from *Lenntech B.V.* as an example. Dimensions are not to scale.

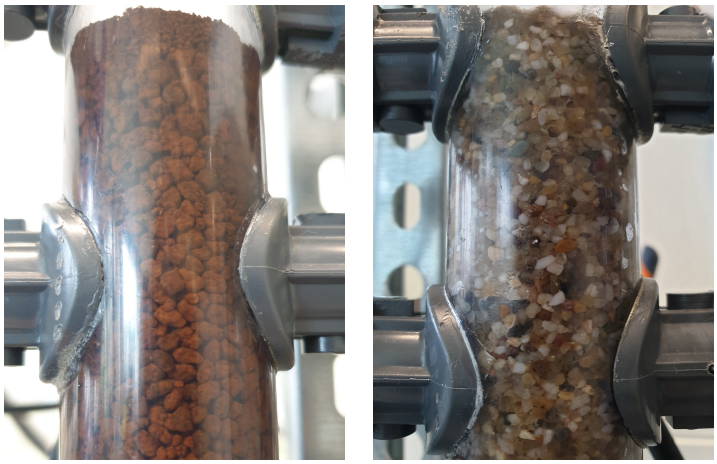

(a) Iron oxide-coated sand. (b) Virgin quartz sand.

Figure A.2: Example of the sands used as a filter media in the columns.

A.2 Hammerflier LOW filter sand activity

Sand used as a filter media from the Hammerflier's DWTP was collected from a pilot-scale filter where no ammonia oxidation occurs. This pilot-scale filter is known as LOW due to its low oxygen concentration (only 5 mg-O_2/L). Thus, even though iron and ammonia are present in the influent of the filter, only iron gets oxidized.

Nevertheless, a batch test was performed to test its activity to ensure that it contains no ammonia-oxidizing microorganisms. Hence, 4 gr of wet sand with 25 mL of water, 75 µL of Trace Elements, and 500 µL of feeding solution (100 mg/L NH_4-N + 87 mg/L of K_2HPO_4) were placed in a horizontal flash shaker at 100 rpm for 8 hours. Ammonia concentration was measured every 2 hours. For an abiotic condition, 4 gr of wet sand were incubated overnight at 50^{o}C in an shaking incubator Certomat BS-1 (B. Braun Biotech International, Germany) at 150 rpm with 50 mg/L of Penicillin-G.

As Figure A.3a indicates, both conditions observed no consumption, proving that the FeOx-coating sand from the LOW filter in Hammerflier had no ammonia-oxidizing microorganisms. The ammonia drop in the first 2 hours is due to ammonia adsorption into the sand grains, as can be confirmed by Figure A.3b when the same experience was repeated with the double amount of sand, leading to an increase in the adsorption capacity.

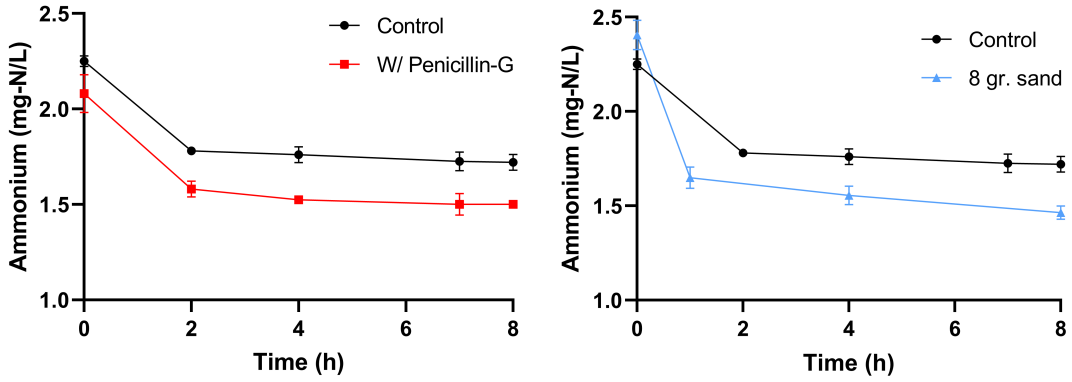

(a) (b)

Figure A.3: Ammonia oxidation activity of Hammerflier LOW filter sand.

A.3 Composition of Trace Elements Solution

The Trace Elements solution used in Sections 3.2 and 3.3 was composed of: 15 g/L of EDTA 4.5 g/L of $ZnSO_4{\cdot}7H_2O$, 0.84 g/L of $MnCl_2{\cdot}2H_2O$, 0.30 g/L of $CoCl_2{\cdot}6H_2O$, 0.30 g/L $CuSO_4{\cdot}5H_2O$, 4.5 g/L of $Na_2MoO_4{\cdot}2H_2O$, 1.0 g/L of H_3BO_3, and 0.10 g/L of KI.

A.4 Columns Sampling Procedure

All samples withdrawn from the columns must be taken very slowly so that the flow rate is not perturbed and the water level in the column remains constant.

The samples are collected with a 2 mL syringe, and the first two full syringes are discharged.

The third sample is used to measure ammonium, nitrite, and nitrate.

Appendix B

Appendix

B.1 Column's ammonia removal capacity profiles

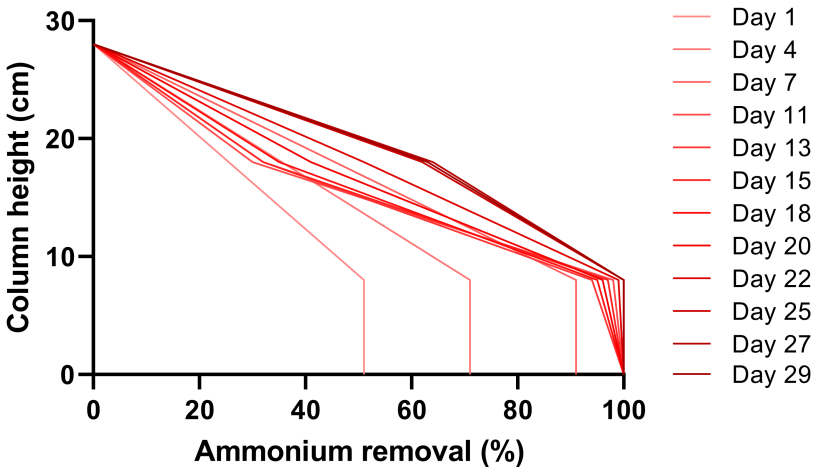

(a) FeOx-coated sand column.

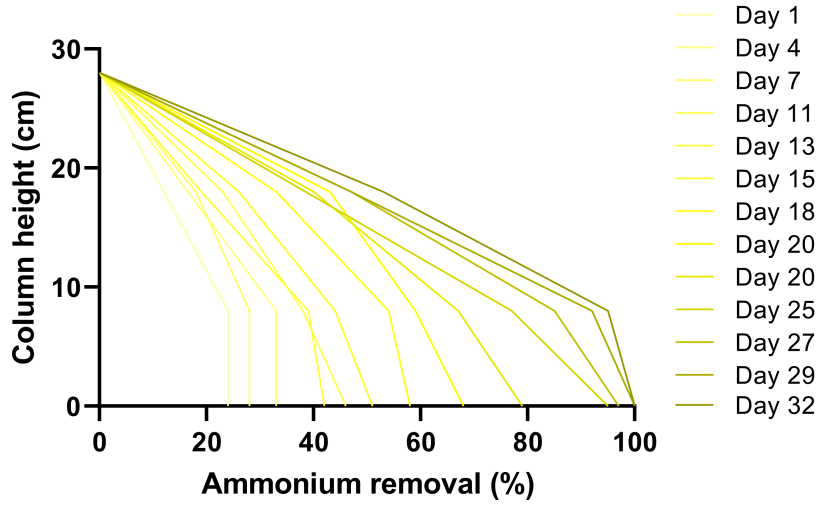

(b) FeOx-virgin sand column.

Figure B.1: Evolution of the ammonia removal capacity profiles of the lab-scale rapid sand filters columns throughout 4 weeks.

B.2 FeOx-virgin sand column's virgin quartz sand's ammonia oxidation activity

A similar procedure from section A.2 was used to test FeOx-virgin sand column's virgin quartz sand's ammonia oxidation activity.

Thus, 4 g of wet sand were sampled from FeOx-virgin sand column, rinsed with tap water, and placed into a horizontal flask shaker (Edmund Bühler GmbH, Germany) at 100 rpm with 25 mL of tap water and 500 µL of feeding solution (100 mg/L NH_4-N + 87 mg/L of K_2HPO_4). The ammonia consumption was measured for 4 hours.

Even though the observed ammonia oxidation rate (0.00266 ± 0.0003 mg-N/h) in Figure B.2 is significantly lower than the activity of the FeOx-coated sand (between 0.0234 ± 0.0019 and 0.0182 ± 0.0009 mg-N/h - see Section 4.3), there is a significant activity ($p<0.0001$) to support the claims on Section 4.2.

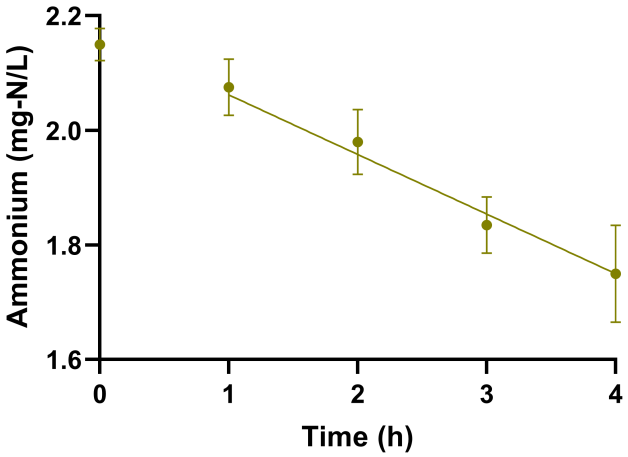

Figure B.2: FeOx-virgin sand column's virgin quartz sand's ammonia oxidation activity.

B.3 Iron(II) addition batch tests

Table B.1: Ammonium consumption rate of control and iron(II) addition every 30 min. The right columns indicate the Standard Deviation (SD) of the replicates and the r^2 of the linear regression used to calculate the consumption rates.

Condition	**Consumption rate [mg-N/(L·h)]**	**SD replicates (mg-N/L)**	**r^2**
Control	0.4698 ± 0.0360	0.0212	0.955
Fe^{2+}	0.3643 ± 0.0166	0.0300	0.984

B.4 Tempol, mannitol, and catalase interference with ammonia oxidation process

Table B.2: Ammonium consumption rate of controls and the four testing conditions - addition of iron, and addition of iron together with ROS quenchers tempol, mannitol, and catalase. The right columns indicate the Standard Deviation (SD) of the replicates and the r^2 of the linear regression used to calculate the consumption rates.

Condition	**Consumption rate [mg-N/(L·h)]**	**SD replicates (mg-N/L)**	**r^2**
Control	0.3521 ± 0.0147	0.0345	0.986
Control + Tempol	0.2718 ± 0.0165	0.0420	0.971
Control + Mannitol	0.2870 ± 0.0232	0.0791	0.950
Control + Catalase	0.3662 ± 0.0153	0.0198	0.986
Fe	0.2781 ± 0.0098	0.0077	0.990
Fe + Tempol	0.2099 ± 0.0142	0.0077	0.965
Fe + Mannitol	0.1762 ± 0.0292	0.1444	0.820
Fe + Catalase	0.2261 ± 0.0077	0.0187	0.991

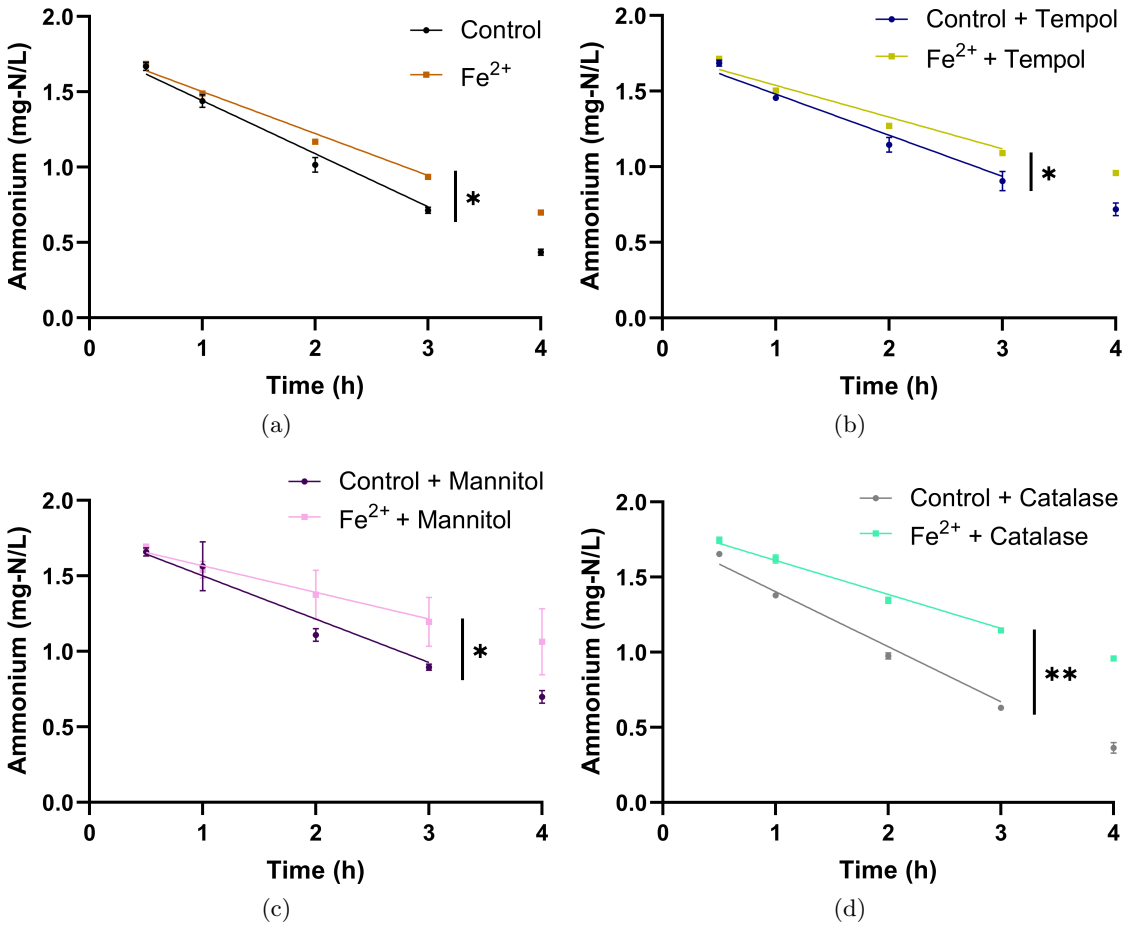

Figure B.3: Ammonia consumption throughout time in the presence of iron alone (a) and coupled with ROS quenchers Tempol (b), Mannitol (c), and Catalase (d). * represents a statistically significant difference of $p<0.05$, and ** a statistically significant difference of $p<0.0001$.

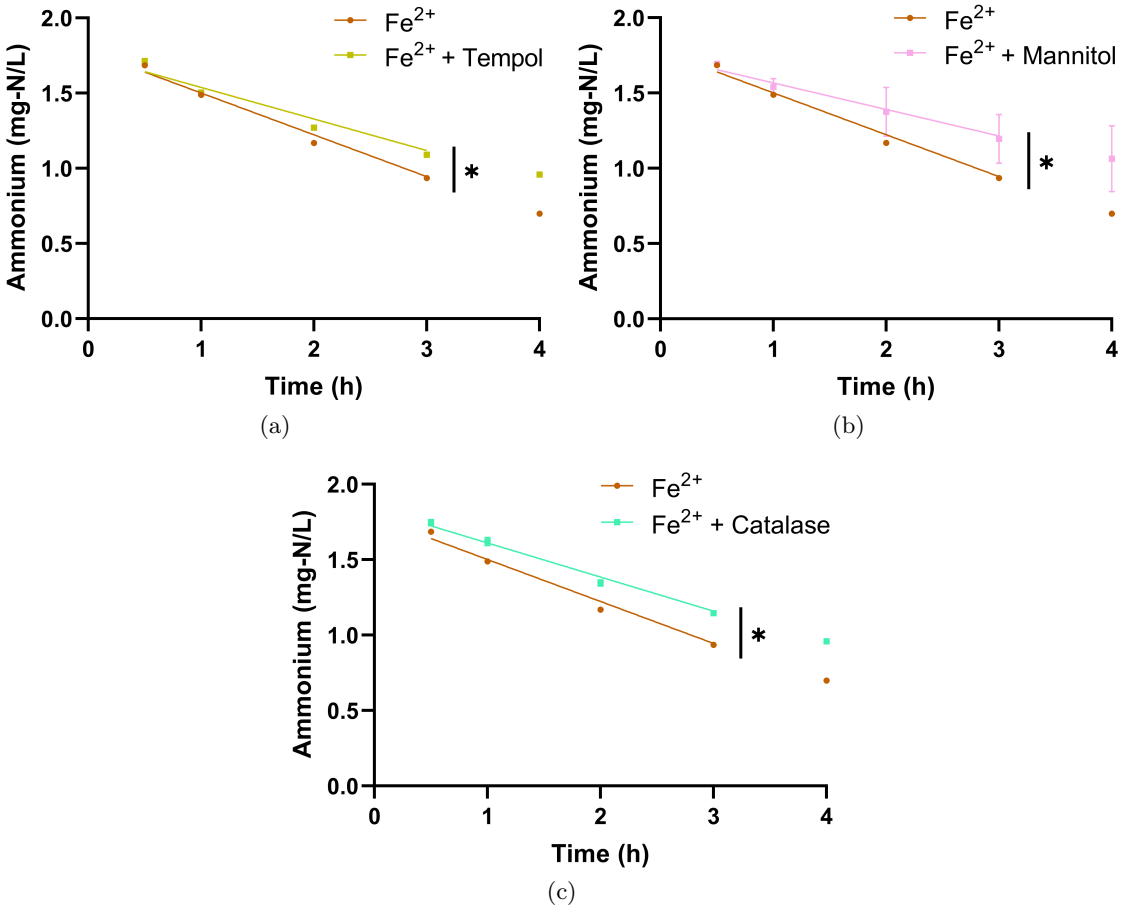

Figure B.4: Ammonia consumption evolution time between the batch with the presence of iron and the batches with presence of iron together with ROS quenchers tempol (a), mannitol (b), and catalase (c). * represents a statistically significant difference of $p<0.05$.

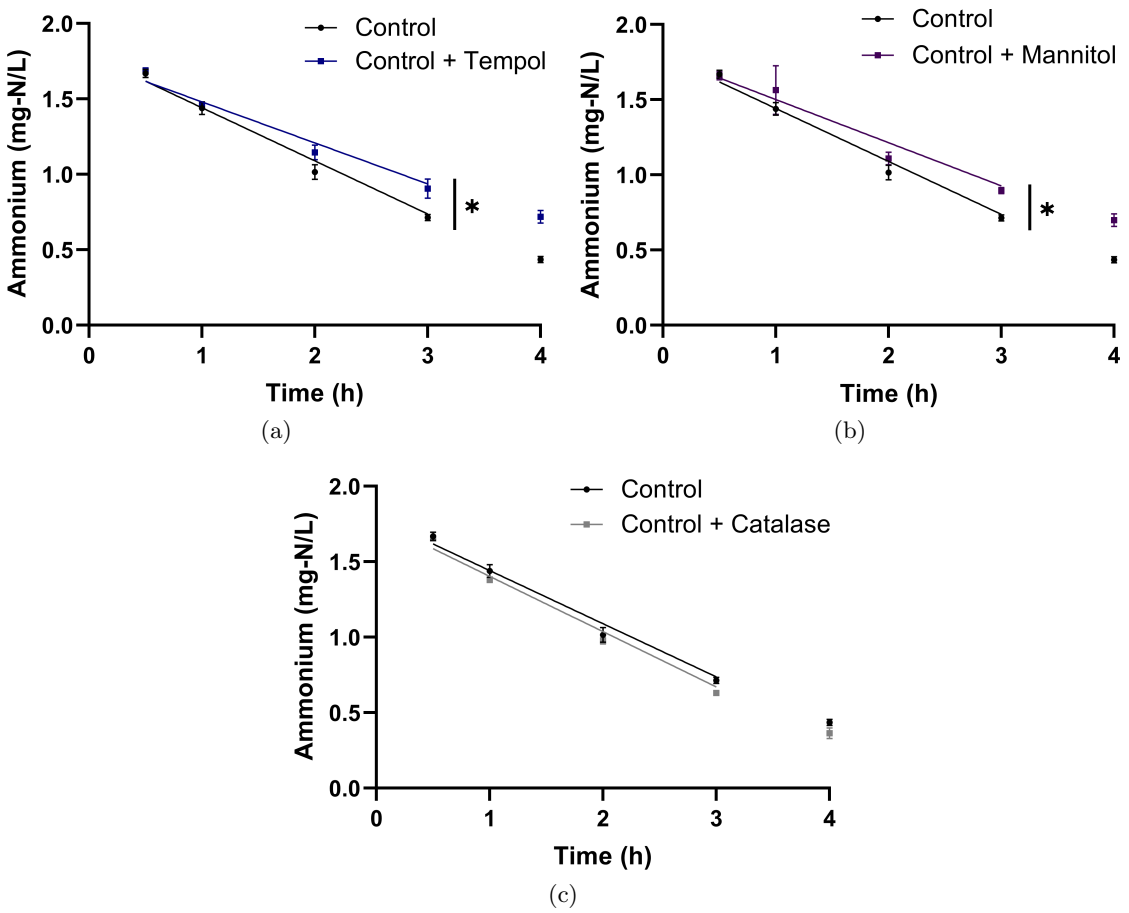

Figure B.5: Differences in ammonia consumption throughout 4 hours of experiment between the control condition and the control with addition of tempol (a), mannitol (b), and catalase (c). * represents a statistically significant difference of $p<0.05$.